

DEVELOPMENT AND CHARACTERIZATION OF ION EXCHANGED MOLECULAR SIEVE HYDROCRACKING CATALYSTS

A Thesis Submitted
In Partial Fulfilment of the Requirements
for the degree of
MASTER OF TECHNOLOGY

By
GOVIND RAM

02802

to the
DEPATMENT OF CHEMICAL ENGINEERING
INDIAN INSTITUTE OF TECHNOLOGY, KANPUR
JUNE, 1977

CME-1977-M-RAM-DEV

I.I.T. CANPUR
CENTRAL LIBRARY

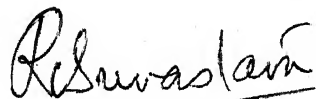
Acc. No. **A 50850**

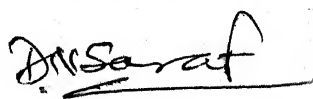
16 AUG 1977

CERTIFICATE

Certified that the work, 'DEVELOPMENT AND CHARACTERIZATION OF ION EXCHANGED MOLECULAR SIEVE HYDROCRACKING CATALYSTS' has been carried out under our supervision and that the work has not been submitted elsewhere for a degree.

June 17, 1977


[R.C. Srivastava]
Assistant Professor
of Physics


[D.N. Saraf]
Professor of
Chemical Engineering

Indian Institute of Technology
Kanpur-208016, U.P.
India

POST GRADUATE OFFICE

This thesis has been approved
for the award of the Degree of
Master of Technology (M.Tech.)
in accordance with the
regulations of the Indian
Institute of Technology Kanpur
Dated. 23.7.77 24

ACKNOWLEDGEMENTS

The author wishes to express his deepest sense of gratitude and sincere regards to Professors D.N. Saraf and R.C. Srivastava for their valuable guidance and time to time discussions and helps provided by them. Their clear and deep insight to the many problems encountered during the period of this work has been a constant source of inspiration and encouragement.

The author is also thankful to Mr. N. Choudhary for allowing to report hydrocracking and ion-exchange data of his Ph.D. work and other helps in this work.

Thanks are also due to Mr. K.K. Rao for time to time help in computer programming. Author is also thankful to all other friends and staffs of chemical engineering, who directly or indirectly helped in completion of this study.

Lastly, but not least, author wants to express his appreciation to Mr. B.S. Pandey for his excellent typing, and Mr. D.S. Panesar for preparing the drawings.

Author

CONTENTS

	List of Tables	...	v
	List of Figures	...	vi
	Abstract	...	vii
CHAPTER			
1	INTRODUCTION	...	1
2	LITERATURE REVIEW	...	5
3	EXPERIMENTAL METHODS	...	21
4	X-Ray ANALYSIS AND LEAST SQUARE REFINEMENT	...	33
5	RESULTS AND DISCUSSIONS	...	47
6	CONCLUSIONS AND RECOMMENDATIONS		76
	REFERENCES	...	78
APPENDIX			
A	X-Ray POWDER DIFFRACTION DATA		83
B	LISTINGS OF COMPUTER PROGRAMS (with brief description of data input)		93

LIST OF TABLES

TABLE		Page
3.1	Properties of Zeolite 13X	22
5.1	Chemical Compositions of Zeolite Catalysts ...	48
5.2	Lanthanum Ion-Exchange Results	49
5.3	Surface Area, Pore Volume, and Pore Size Distribution Data ...	60
5.4	Unit Cell Parameters of Zeolite Catalysts ...	64
5.5	Final Atomic Parameters ...	65
5.6	Interatomic Distances and Angles for Different Zeolite Samples	68
5.7	Average Bond Lengths and Angles for the Framework of Zeolite Samples	69

LIST OF FIGURES

FIGURE		Page
3.1	Sodium Calibration Curve	26
3.2	Experimental Set-up for Hydrocracking	29
4.1	Idealized Projection of Sodalite Unit with Atom Nomenclature ...	32
4.2	Section through abcdefghij in Figure 4.1 Showing the Relative Position of Cation Sites ...	32
4.3	Three Dimensional Model of the Framework Showing Supercage and Cation Sites	33
5.1	Thermogravimetric Curves for NaX-100, LaX-58, LaX-96, LaX-79 and NiX-80 Catalysts	52
5.2	Differential Thermogravimetric Curve for NaX-100, LaX-58, LaX-96, LaX-79, and NiX-80 Catalysts ...	54
5.3	Variation in the Number of Water Molecules with the Degree of Exchange	56
5.4	Trace of DTA Thermograms for LaX-58, LaX-79, LaX-96 Catalysts	58
5.5	Plot of Per Cent Conversion vs Different Degree of Lanthanum Exchange, for Hydro- cracking Reaction ...	61

ABSTRACT

Zeolite 13X was ion-exchanged with rare earth (La^{3+}) or transition metal cations (Ni^{2+}). The catalysts thus developed, for hydrocracking of Assam crude residue, were characterized by DTA, TG, surface area, pore volume, pore size distribution and x-ray analysis. In x-ray analysis least square refinement of LaX catalysts, based on the powder method was done to study the effect of degree of lanthanum exchange on the site occupancy and selectivity. LaX-96 was established to be most suitable catalyst for hydrocracking of the reduced crude. Performance of NiX-80 sample was not upto the expectation perhaps due to partial loss of structure of the catalyst as shown by surface area measurements and x-ray analysis data. Na^+ ions situated at site I were found to be most difficult to ion-exchange. La^{3+} ions preferred site II and their next preference was shown to be for site I'.

CHAPTER 1

INTRODUCTION

The discovery of zeolite molecular sieves can be termed as revolution in chemical industry. We can realize the magnitude of interest shown by scientists and engineers by the fact that from the first industrial research in 1948 until the end of 1972, over 7000 papers have been published and 2000 U.S. patents obtained dealing with zeolite science and technology.

Synthetic molecular sieves are crystalline, hydrated aluminosilicates of group I and group II. Due to many unique properties of zeolites they are being used in a great variety of applications such as hydrocarbon conversion catalysts, recovering radioactive ions from waste solutions, separating hydrogen isotopes, solubilizing enzymes, carrying active catalysts in the curing of plastics and rubber, transporting soil nutrients in fertilizers, cryopumping, removing carbon-dioxide and sulfur compounds from natural gas, separation of n-paraffins, removal of atmospheric pollutants such as sulfur dioxide etc.

Petroleum refining industry has been very much benefitted by the use of zeolites as cracking catalysts. Synthetic zeolites have completely replaced the amorphous silica-alumina catalysts used previously for cracking processes. In our country the demand for diesel and kerosene oil is much more compared to that

of the gasoline therefore hydrocracking of reduced crude is a more suitable process. For hydrocracking zeolite catalysts are preferred due to higher activity, more liquid product formation and less gas and coke production. Recently Choudhary and Saraf [1] have published a review on hydrocracking catalysts.

Zeolites have unique property that by simple methods one can change their catalytic and adsorption capabilities to suit the specific purpose for which they are going to be used.

Of all the methods mentioned above ion-exchange is very simple and is most extensively used. In zeolite 13X, to which the present work is confined, Na^+ ions serve the purpose of neutralising the negative charge of aluminum-oxygen tetrahedra. These Na^+ ions can be easily exchanged with some other mono-, di-, or tri-valent cations, without seriously altering the original framework structure. Using this method we have obtained uniform and extremely fine dispersion of metal ions throughout the structure of catalyst which is not possible by bulk adsorption or impregnation methods [2].

A catalyst cannot be fully described simply by its chemical formula or name. Importance of extensive characterization of its physicochemical properties is well recognized. It becomes more important in the case of molecular sieve zeolites because ~~here~~ structure plays a very prominent role in their catalytic activity.

Commonly used characterization methods are surface area measurement, pore volume and pore size distribution, differential thermal analysis (DTA), thermogravimetric analysis (TGA) etc. X-ray diffraction analysis and infrared absorption analysis are also being used for this purpose. These two methods give an idea about the internal structure of the catalyst at molecular level. X-ray analysis can be used to determine the structure of the catalyst, cation positions bond angles and lengths etc. By infrared analysis we can locate even small molecules like water which may not be regularly spaced and hence may not be detected by x-ray diffraction methods. Acidic or basic nature of the catalyst also affects its catalytic activity. So strength of acid sites and their type (Brownsted or Lewis) should also be determined in the case of acidic catalyst like molecular sieves.

Objective of Present Investigation:

The aim of present investigation was to study the changes in the thermal stability, catalytic activity and structure of the catalyst (zeolite 13X) on exchanging it with other cations. Catalytic activity was tested for hydrocracking reaction on Assam crude oil residue.

Rare earth metals like lanthanum (La^{3+}) and transition metals like nickel (Ni^{2+}) were used to replace Na^+ ions of the parent zeolite 13X. This type of a catalyst is bifunctional in nature. Here La^{3+} or Ni^{2+} ions act as hydrogenating catalysts

and the rest of silica-alumina crystalline structure acts as cracking catalyst. Lanthanum and nickel ions not only act as hydrogenating catalyst but also help in cracking phenomena by reducing the coke formation at the active sites of the catalyst.

In x-ray analysis not only the routine determine of crystallinity, interplaner spacings, unit cell constants etc. were carried out but also the structure changes were investigated using the powder diffraction data and least square refinement method, for both original and ion-exchanged forms of zeolite. For lanthanum exchanged zeolite X there is no information available in the literature regarding the change in the location of cation positions and occupancy factors with varying degree of exchange. This was attempted in the present study.

The reported methods of improving thermal and catalytic properties of the zeolite, the published work in using x-ray analysis, differential thermal analysis, thermogravimetry etc. have been reviewed in Chapter 2 of this dissertation. Chapter 3 deals with the experimental methods used. In Chapter 4 outlines of the x-ray analysis method including least square refinement programme and bond lengths and angle calculation procedures are described. Last two chapters are devoted to results, discussions, conclusions and recommendations for extension of this work.

CHAPTER 2

LITERATURE REVIEW

2.1 Activity and Thermal Stability Improvement Methods:

Since the development of zeolite molecular sieves as catalyst and adsorbent in chemical processes, a lot of work has been done to improve their thermal stability, catalytic activity and selectivity. Different methods developed are (1) dealumination, (2) decationation, (3) addition of proton source and (4) ion-exchange or active metal loading. Whereas decationation and dealumination have been recently developed ion-exchange or active metal loading has been in use for a long time. Not much work is done in the field of proton source addition.

The fundamental unit of zeolite structure is a SiO_4 or AlO_4 tetrahedron. In case of AlO_4 tetrahedron, Al^{3+} being trivalent, a deficiency in electrical charge is produced which is neutralized locally by the presence of an additional positive ion (generally one of the alkali metals or alkaline earths). In zeolite X and Y these are Na^+ ions. These cations are loosely attached to the tetrahedral oxygens.

2.1.1 Dealumination:

Removal of tetrahedral aluminum atoms from framework by complexing agents is called dealumination. By this method Si/Al ratio is increased which results in better thermal

stability. But removal of aluminum is more difficult than that of sodium cations because while the later is loosely attached to the oxygens, the former takes part in the building blocks of framework structure. Kerr [3] succeeded in removing Al from the frame work of Na-Y by extraction with chelating agent ethylene diamine tetraacetic acid (H_4 EDTA). He observed that removal of up to 50 per cent of the aluminum yields highly crystalline product of increased sorptive capacity and improved thermal-stability. This extraction is accomplished in two stages. In the first stage, atoms from weak acid sites are removed and only after completion of this step, strong acid sites start loosing their Al atoms in the second stage. It is well established now that the sites vacated by aluminum are filled by silicon atoms [4]. Recently Peri [5] has shown by infrared study of dealuminated faujasite that during formation of ultrastable faujasite, Al migrates from tetrahedral sites in the aluminosilicate framework to cation positions out side the tetrahedron. He has also indicated that the silicon replaces the lost aluminum through recrystallization of the framework. Besides increasing the thermal stability, dealumination also increases catalytic activity and acidity is redistributed. Strength of Brownsted acid sites are increased without changing their total number [6,7].

2.1.2 Decationation:

In this method zeolite is ion-exchanged with thermally

decomposable ammonium ions. After ion-exchange, zeolite is heated to liberate ammonia gas and proton containing intermediate is produced. Kerr [8] has shown that the product obtained depends on the process of calcinations. By shallow-bed calcination at 760 torr and 500°C, with efficient removal of ammonia-produced, one gets hydrogen zeolite. When ammonia removal is impeded due to bed geometry than the yield is an ultrastable faujasite. Although both have high catalytic activity, ultrastable faujasite is more thermally stable than H-type [9]. However, Ambs and Flank [10] have concluded, on the basis of limited data, that the thermal stability of synthetic faujasite is dependent only on the level of sodium present.

2.1.3 Proton Source Addition:

Alkalimetal zeolite's acidity can be improved by the additions of a proton source such as hydrochloric acid, carbondioxide or propyle chloride [11, 12]. In acid treatment, care has to be taken of the pH, otherwise structure of zeolite may collapse. The improvement in acidity due to the presence of carbon dioxide is explained by the presence of Ca^{2+} ions, impurities in the zeolite. Propyl chloride's action is complex and intriguing because of the suppression of the catalytic activity of the active catalysts like HX and CaX

2.1.4 Ion-Exchange:

Zeolites undergo reversible cation exchange. This is one of their most important properties. Ion-exchange changes the electric field inside the zeolite structure [13] which in turn modifies the sorptive and catalytic properties. In 1850 Way [14] had reported ion-exchange property of the zeolites. Since then a lot of work has been done in this field [15,16, 17]. Based on these works, effects of various factors on the degree of exchange are summarised and given below.

1. Operating temperature: Higher temperature favours higher degree of exchange.
2. Concentration of cation species in solution: Zeolite preferentially selects the ions with highest charge at low total normality and ions with lowest charge at high normality.
3. Solvent: Decrease in dielectric constant of solvent decreases rate of ion-exchange and selectivity. However aqueous solutions have been used in most of the experiments.
4. Anionic species such as hydroxyl ions associated with cation: As hydrated cation radius is greater than that of dehydrated one, association of water molecules with cations decreases the degree of ion exchange.
5. Nature of Zeolite: Zeolite structure and silica/Alumina ratio also affects ion-exchange. For high

degree of ion exchange silica/alumina ration should be low.

6. Nature of cation species: Size of the cation, its valency or charge also control the degree of ion exchange. For better ion-exchange, cation radius (both hydrated and dehydrated) and valency should be smaller i.e. monovalent cations give more complete exchange than polyvalent cations.

A number of ion-exchange studies have been done by Barrer and Rees [18, 19; 20] and Sherry [21] on zeolites X and Y. In these works they have demonstrated that alkali metal cations with large radii such as Cs^+ and Rb^+ cannot completely replace all the sodium ions in NaX or NaY. Explanation for this partial exchange is that Na^+ ions occupy different sites. Ions located in the large cavities or supercages are easily exchanged compared to those located in the smaller cavities. Rare earth ion exchange in zeolites X and Y was reported by Sherry [21] in 1966. For La^{3+} exchanged sample he has shown that at 25°C , 16 Na^+ ions per unit cell, located at the center of hexagonal prism, could not be replaced with La^{3+} . For almost complete exchange (99 per cent), temperature was raised to 100°C and time required was 13 days. High temperature stripped off the water molecules from the ion and thus by reducing its radius from 3.96 \AA (hydrated) to near about 1.15 \AA (dehydrated) enabled it to enter through the 'windows'

into the sodalite unit. So the exchange of polyvalent ions is distinguished by 2 steps - one being many orders of magnitude slower than the other. Slow step involves exchange of relatively inaccessible 16 Na^+ ions per unit cell. It is not necessary that entering ions should occupy same sites or should have the same site distribution. This fact was illustrated by Sr^{2+} and Cs^+ ion-exchange studies, [17].

There are substantial differences in the nature of exchange of sodium ions in zeolites X and Y by other cations [17,21,22]. Equilibria (level of exchange attained), selectivities and thermodynamic aspects are quite different. The thermodynamic preference for the sites in the large cages of the more aluminous zeolite X, with the exception of Li^+ , decreases with increasing ionic radius, where as in the case of zeolite Y the thermodynamic preference decreases with increasing ionic hydration energy.

2.2 Characterization Methods:

2.2.1 X-ray Analysis:

X-ray analysis has been very extensively used for crystal structure determination. Zeolite structure was also delineated by using this technique and applying Pauling's rule [23] for complex ionic structure. The fundamental unit in silicate structures is a tetrahedral complex consisting of small cations, such as Si^{4+} , in tetrahedral coordination with

4 oxygen atoms. The Al^{3+} can also be linked tetrahedrally with oxygens when extra negative charge is balanced by the presence of one cation such as sodium per tetrahedra. The ways in which the tetrahedral groups may be linked by the sharing of oxygen atoms, variation in chemical compositions, structure differences etc. result in a large number of compounds called zeolites. For systematic ordered naming of zeolites their structural classification was proposed by Smith [24] and Fischer and Mier [25]. Based on framework topology, zeolites were divided in 7 groups. Within each group, the zeolites have a common subunit of structure which is a specific array of $(\text{Al}, \text{Si})\text{O}_4$ tetrahedra. Mier named the 4 membered or six membered rings as 'secondary building units' (SbU) and SiO_4 and AlO_4 tetrahedra as primary units.

As for example, zeolite A comes under group 3 and zeolite X, Zeolite Y, and faujasite are members of group 4. Secondary building unit for group 4 members are double six membered rings or hexagonal prisms where as for group 3 secondary building units are double four membered rings. First of all the prototype faujasite mineral was described by Damour [26] in 1842. Framework topology of synthetic zeolites X and Y were shown by X-ray powder method to be similar to that of faujasite [27,28]. Differences between Y and X zeolites are due to their different chemical compositions, the former type contains 48 to 76 Al atoms per cell whereas the latter has 77 to 96.

Silica/Alumina ratio is higher in zeolite Y (1.5 to 3) compared to that in type X (1 to 1.5) [29]. Due to high silica content, zeolite Y has lower value of cell constant (24.61 to 24.85 \AA). A unit cell of both X and Y zeolites contain 192 (Silica, Alumina) O_4 tetrahedra. The void volume is largest in X and Y types among known zeolites and amounts to about 50 volume per cent of dehydrated crystals.

Atom sites and their generally accepted nomenclature have been reviewed by Smith [30]. Earlier workers [31, 32] used sites notations different from the one being used now. (These sites are shown in Figure 4.1 and are described in chapter 4).

The structure of mineral faujasite was determined by Bergerhoff et al. [33] in 1958. Broussard and Shoemaker [31] established the structural similarity of zeolite 13X and mineral faujasite. Crystal structures of 4A and 5A zeolites have been discussed by Reed and Breck [34] and by Barrer [35]. From these works it was established that main building block for both type X and type A zeolites is a 'sodalite unit'. The sodalite unit is a truncated octahedron having 36 edges, 24 vertices, 6 square faces and 8 hexagonal faces. At each vertex one silicon or aluminum atom (both called T atom) is placed. The mid points of the edges of sodalite unit are occupied by oxygen atoms. Thus, a sodalite unit contains 24 (Si, Al) ions interconnected with 36 oxygen anions. Shoemaker

et. al [31] have also demonstrated that in the 4A and 5A molecular sieves, these sodalite units are arranged in a simple cubic array, with each sodalite unit connected to its neighbour by four bridge oxygen ions. But in 13X, sodalite units are in tetrahedral coordination (diamond array) with each sodalite unit connected to its neighbour by six bridge oxygen ions.

The dehydration of zeolites may produce distortions in the shape of the tetrahedra. Olson and Dempsey [36] have dealt with this aspect in detail supported by quantitative evidence. Hydrated specimens have more uniform T-O distances and O-T-O angles than dehydrated ones.

All of the earlier workers [27,28,31,32,33] have assigned space group $Fd\bar{3}m$ to the faujasite type structure but Olson [37] has recently demonstrated from single-crystal x-ray analysis that hydrated Na-X belongs to the non-centrosymmetric space group $Fd\bar{3}$. He distinguished tetrahedra having silicon at the centre from that having aluminum. Whereas in the earlier work of Shoemaker which was based on powder data, 16 sodium atoms were at site I and 32 sodium atoms at site II, Olson distributed them in the order of 9 Na^+ at site I, 8 at site I' and 24 at site II. Out of a total of 80, about 32 sodium atoms could not be located in both the works.

Several investigations were carried out to find various aspects of order-disorder in zeolites. When $Si/Al > 1$, all

faujasite type materials have either short range or long range disorder. At low temperature disorder is less compared to high temperature. A detailed discussion of order-disorder has been given by Dempsey [13] and Dempsey, Kuhl and Olson [38]. In these works they have also discussed, how with Si/Al ratio variations, different modifications in the structure occurs. Dempsey et al. [38] have suggested that the variation in cell dimensions supported the concept of Si, Al disorder in the faujasite type zeolites. They have plotted unit cell constants as a function of aluminum content and obtained straight line relationship with discontinuities at 52, 64 and 80 Al atoms per cell. Last two discontinuities were explained in terms of rearrangement of T atoms and the first one was ascribed to possible formation of amorphous silica in the more siliceous bulk compositions.

Ion-exchanged forms of zeolites have also been studied by x-ray analysis. Presence of water and sorbed molecules affect the positions occupied by exchanged cations. Different data are available in the literature for hydrated, partially dehydrated and dehydrated forms of ion-exchanged zeolites. Ideally, the water molecules in a zeolite should exist as discrete molecules which can be removed easily by heating. In practice, however, the water molecules form hydration complexes with exchangeable cations and interact electrostatically with framework oxygens. But for monovalent cations these hydration

complexes are weakly bonded and dehydration is relatively easy. This fact was supported by Eulenberger et al. [39] based on their data for dehydrated K-Y (Powder technique) and K-faujasite (single crystal technique). The potassium and silver ions occupied the same sites, namely, I, I' and II but with different occupancy factors. In all these Y type of dehydrated zeolites, about 58 cations per cell are required to balance Al atoms and this is in agreement with total occupancy estimated from x-ray analysis [39, 40, 41]. Due to considerable problems in placing 86 cations per unit cell very few data have been published on the location of monovalent cations in dehydrated X zeolites. Breck [42] placed 16 in I, 32 in II and 38 in site III. But still there is controversy, whether site III is occupied or site I and I' are occupied simultaneously as in the case of zeolite Y [30].

Polyvalent exchanged forms of zeolites have also been studied. Nickel exchanged faujasite structure has been reported by Olson [43] and he has pointed out the changes in bond lengths and bond angles by ion-exchanging sodium with nickel. Other workers [44-47] have also observed that Ni causes distortion and disorder in zeolite X lattice resulting in partial loss of crystal structure. Serpinskii et al. [47] have studied adsorption of propane on nickel exchanged type X zeolites. They explained the decrease in adsorption volume with increase in nickel exchange in terms of partial loss in crystal

structure and some other factors. In his single crystal study of Ni-faujasite Olson [43] assigned 10.6 nickel ions at site I, and 3.2, 1.9 and 6.4, ions respectively at sites I', II' and II which indicates that nickel ions preferably occupy site I. Gallezot et al. [48] have studied different degrees of cobalt exchanged forms of zeolite Y. They have shown that in partially dehydrated samples, (at 200°C) Co^{2+} ions mostly occupy sites I' and II' and are coordinated by a tetrahedron built on 3 oxygen atoms of zeolite frame work and one from residual water molecule. When strongly dehydrated at 600°C 80 per cent of localized Co^{2+} ions occupy site I and are coordinated by an octahedron formed with 6 oxygen atoms of the hexagonal prism. Behaviour of Co^{2+} ions and Ni^{2+} ions have been found to be similar. Recently Zhavoronkov [49] put forward a theoretical method of determining di- and trivalent cation distribution in zeolite Y considering ionic - covalent model of zeolite structure. Based on electrostatic parameter, i.e. ratio of square of formal charge and cation radius, and covalent parameter i.e. difference between ionization potential and heat of dehydration, he has come out with a list of divalent and trivalent cations having priority for site II. His results agree fairly well with the experimental data.

Due to their importance in the field of catalysis, trivalent cation exchanged zeolites have been investigated very extensively. Cerium and Lanthanum exchanged zeolite 13X were

analysed by Olson et al. [32]. Single crystal was used for cerium exchanged faujasite and powder x-ray data for lanthanum exchanged 13 X zeolite. They found out that all rare earth ions in freshly exchanged natural faujasite are contained with 13 Å diameter large cavity, with partial occupancy of the site located in the centre of the 12 tetrahedra ring, i.e. site V. However, lanthanum ions occupy three sites I', II, and V having 12, 17 and 4 lanthanum respectively. In the calcined sample of exchanged 13X, all lanthanum ions move to site I'. Effect of different degrees of dehydration upon lanthanum exchanged 13X structure has been reported by Smith et al. [50]. At room temperature the lanthanum atoms preferred sites I', II and V. At 425 and 735°C in helium stream, the lanthanum ions were found to occupy sites I, I' and II. Smith et al. concluded that lanthanum atoms tend to occupy sites I and II when X-zeolite is strictly dehydrated and dehydroxylated and that they prefer site I' when some residual molecules are available, which was the case with the sample of Olson's calcined 13X. In their further work Bennet and Smith [51,52] demonstrated that in dehydrated lanthanum exchanged faujasite as high as 11.8 lanthanum atoms are occupying site I and the rest are at sites I' and II. From the correlation of above results with those obtained by Rabo et al. [53] using infrared method, it was proved beyond

reasonable doubt that the positions of cations depend on even small quantities of residual water molecules. Hydrated lanthanum exchanged faujasite structure data was also published by Smith and Bennet [54]. In this case they could locate only 3.3 atoms at site I' compared to 12 atoms in the case of hydrated lanthanum exchanged zeolite-X [32]. Olson [42] made an important suggestion that in hydrated systems, cations only occupy site II when there are 3 Al atoms in the 6-ring to provide a favourable electrostatic environment. Since faujasite and Y zeolites probably do not have more than 2 aluminium atoms in almost all 6-rings, ions should only occupy site II in x-zeolite. This suggestion was supported by experimental data. There is no data available in literature for the effect of degree of ion-exchange on cation positions and site occupancies of lanthanum exchanged zeolite X.

2.2.2 Other Characterization Methods:

As zeolite catalysts are some times used at very high temperature the thermal stability of zeolites has been studied by usual differential thermal analysis (DTA) and thermogravimetry. Grim [55] has published detailed discussions of the theory and technique of thermal analysis. Barrer et al. [56] have applied these methods in the field of zeolites. DTA determines the temperature at which thermal reactions take place within the sample. Thermogravimetric analysis (TGA)

measures the loss in weight of substance as it is heated to elevated temperature. A series of cation exchanged forms of zeolite X have been studied by means of this method and water adsorption equilibrium measurements. Barrer et al. [56, 57] have observed for strontium exchanged zeolite X, a certain amount of hysteresis or irreversible adsorption phenomenon. DTA curve of zeolite X indicates a continuous loss of water over a broad range starting from slightly above room temperature to about 350°C . Breck et al. [58] found out that at 772 and 993°C exothermic peaks were present which indicated decomposition followed by recrystallization of the zeolite. After heating for 36 hour at 760°C , the zeolite becomes amorphous in structure and recrystallizes to a carageite-like phase at 800°C and to nephedine-like phase at 1000°C . Zeolite Y, because of high silica content, is found to be more thermally stable. It has also been reported [56, 57, 58] that zeolite Y has broad endothermic peak with maximum at 208°C and an exothermic peak at 790°C . Even after prolonged heating in air at 760°C no structural change was noticed, but at 800°C the structure collapsed to an amorphous residue. Rare earth exchanged zeolite are found to be stable even above 1000°C .

Hydrocracking processes have been reviewed very extensively by many workers [60, 61, 62, 63]. Recently Choudhary and Saraf [1] have reviewed hydrocracking processes and

catalysts used in great detail. Choudhary [64] has studied hydrocracking of Assam crude residue using La-X catalysts with varying degree of exchange. He has also investigated use of Ni-X catalyst on the same reaction system.

CHAPTER 3

EXPERIMENTAL METHODS

3.1 Ion Exchange:

Synthetic molecular sieves type X (NaX) supplied by Linde Division of Union Carbide were used to develop the ion-exchanged form of catalyst. The physico-chemical properties of original molecular sieves are given in Table 3.1. NaX catalyst was in the form of pellets of size 1/16 inch diameter. Sodium ions in parent NaX were replaced with the rare earth or transition metal cations. In rare earth group lanthanum (La^{3+}) ion and in transition metal group Nickel (Ni^{2+}) ion were selected due to their known superior hydrogenating properties.

For the preparation of lanthanum exchanged zeolite (LaX), pellets of NaX were slurrified in aqueous solution of lanthanum chloride. Ion-exchange was performed in constant temperature bath maintained at 70°C and shaken continuously. To ensure maximum possible exchange, the salt solution was used four times in excess of the requirement of La^{3+} cations for complete exchange. In one batch 12 grams of zeolite was equilibrated with 200 ml of normal solution of lanthanum chloride. When (after several days) equilibrium was reached, the catalyst was filtered and washed by adding distilled water to remove soluble salt adhering to the pellets. For lower level of

TABLE 3.1: PROPERTIES OF ZEOLITES 13X

Type X (SK - 20) ^α	
Chemical Formula	$\text{Na}_{86}[(\text{AlO}_2)_{86}(\text{SiO}_2)_{106}] \cdot x\text{H}_2\text{O}$
Properties of Pellets	
Nominal pore diameter	10Å
Extrudate dimension	1/16 inch
Apparent bulk density	38 lbs/cuft.
Crush strength	12 lbs
Equilibrium H ₂ O capacity	28.5 per cent weight
Heat of adsorption (Max)	1800 Btu/lb H ₂ O
Molecules adsorbed	< 10Å effective diameter
Molecules excluded	> 10Å effective diameter
	e.g. (C ₄ F ₉) ₃ N.

^αBulletin F-23, Union Carbide Corporation, Molecular Sieve
Department, 270 Park Ave, New York, N.Y. 10017, U.S.A.

ion-exchanged zeolite was allowed to equilibrate with a calculated amount of cations in the solution. Number of equilibrations required was large for higher degree of exchanged. To accelerate the rate of residual ion-exchange, intermediate heat-treatment was given to the partially exchanged zeolite sample. As pointed out earlier heat treatment forced the migration of sodium ions from inaccessible sites to more accessible ones. The heat treatment consisted of heating the partially exchanged zeolite ^{to} 300-350°C for about one hour.

Similarly nickel exchanged zeolite (NiX) was prepared by using nickel nitrate as salt solution. To achieve more than 50 per cent exchange, several equilibrations were required.

To evaluate the extent of exchange achieved the concentration of sodium ions present in equilibrating solution was determined. The systronic Flame photometer type 121 MK-1 was used to measure the concentration of sodium ions in the filtrate. A calibration curve was obtained by using several stock-solutions of known Na^+ ion concentration and plotting this concentration against deflection obtained in Flame photometer. Experiments were conducted to check whether the presence of lanthanum or nickel ions in different concentration affected the result of flame photometry. Fortunately it was found that deflection reading was independent of concentration of lanthanum or nickel ions. Therefore the same calibration curve for pure

sodium (Figure 3.1) was used to convert the deflection readings into equivalent concentration of sodium in milligrams per litre for both the systems. For calculation of degree of ion-exchange, it was assumed that total number of sodium milliequivalent in filtrate was replaced by equivalent amount of lanthanum (or nickel) in the zeolite. Remaining sodium ions in the zeolite structure were calculated by subtracting this amount of sodium ions in filtrate solution from total number of sodium ions present in the original zeolite. Degree of ion-exchange was defined as $\left[\frac{3 \text{ La}^{3+}}{(3 \text{ La}^{3+} + \text{Na}^+)} \right] \times 100$ and $\left[\frac{2 \text{ Ni}^{2+}}{(2 \text{ Ni}^{2+} + \text{Na}^+)} \right] \times 100$ respectively. Here La^{3+} , Ni^{2+} and Na^+ are the milliequivalent of cations present in the zeolite. Notations used for representing ion-exchanged samples are like LaX-96, meaning a X type zeolite sample in which 96 per cent of exchangeable sodium ions have been replaced by lanthanum.

3.2 Characterization Methods:

3.2.1 X-ray Powder Analysis:

For x-ray analysis pellets were ground into the form of fine powder which passed through 300 mesh but was retained by 400 mesh. Too fine powder results in broadening of peaks and coarse powder may not provide enough particles oriented in all directions which is the basic assumption in x-ray powder analysis. For getting diffraction pattern of powdered zeolite samples, GE-XRD-5 and -6 Diffractrometers were used. The set-up

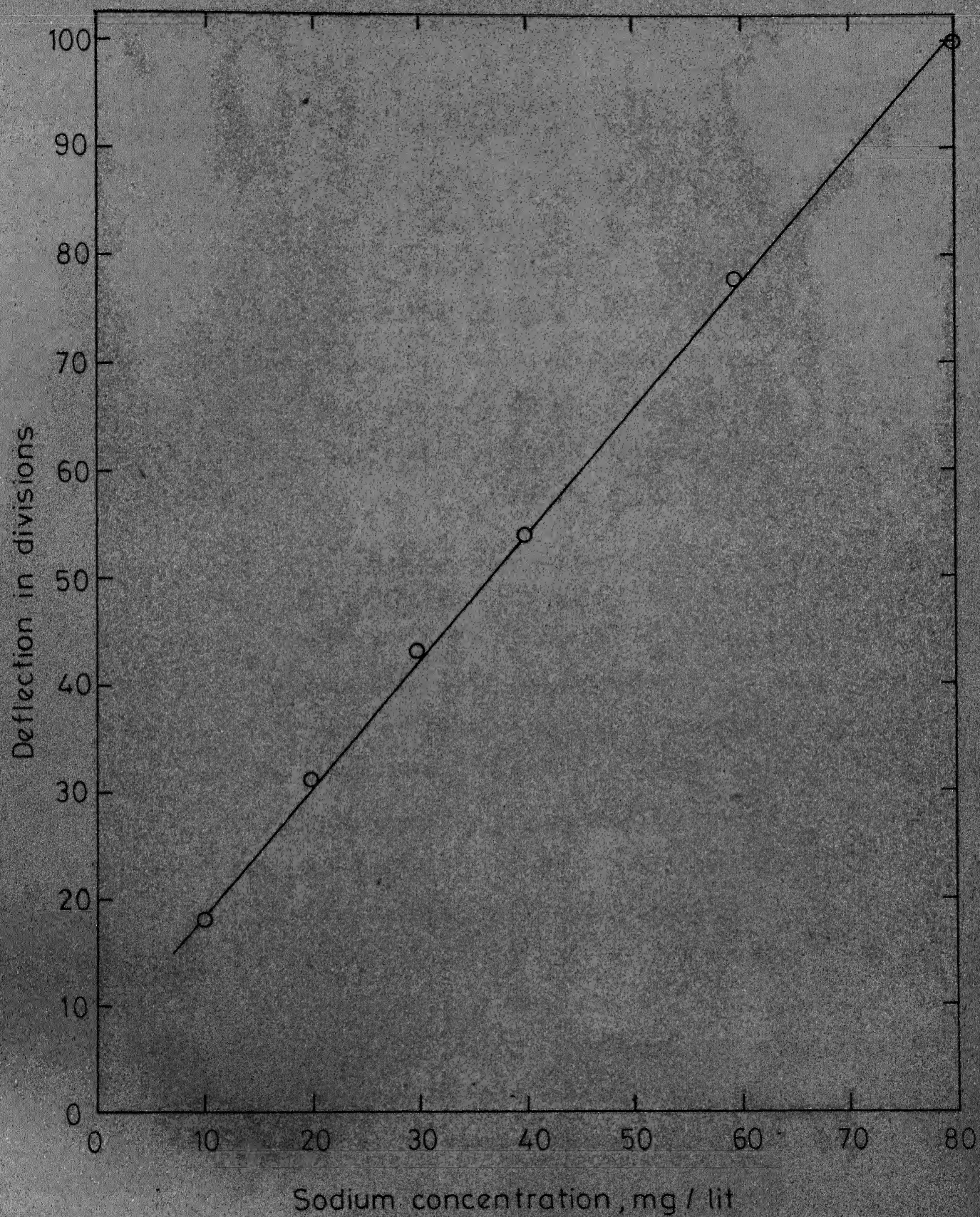


Fig.3.1- Sodium calibration curve.

consisted of XRD-6 x-ray generator, SpG-4 Detector System, SpG-2 Diffractometer and xenon filled proportional counter.

Small amount of sample was placed in the cavity of plastic sample holder and upper surface was smoothened by pressing and removing the excess. Then this sample holder was mounted on the diffractometer. Copper ($K\alpha$) radiation ($\lambda = 1.5418 \text{ \AA}$) was used. β -radiation was cut off by using the Ni filter. In preliminary studies samples were scanned at a rate of $2^\circ/\text{min}$ and the chart was moved at a speed of $1''/\text{min}$. Receiving slit used was of 0.1° width. 30 KV power and 20 mA current were used for generation of x-rays. Standard permaquartz sample was used to check the zero error. To get more accurate intensity data and peak position, point to point intensity data were noted down by using the scalar and counter. Each peak was divided into 5 to 10 intervals and number of counts were recorded at these points by setting the timer for 20 sec. These counts were plotted against 2θ and the area under the curve was obtained to get integrated intensity of each peak. Percentage relative integrated intensities were obtained by dividing all intensity data with the one having highest value and then multiplying with 100. This raw intensity data were corrected for Lorentz, and polarization corrections and calculations proceeded with as described in the subsequent chapter.

3.2.2 Other Characterization Methods:

Differential Thermal Analysis and Thermogravimetry:

Differential thermal analysis (DTA), as mentioned in previous chapter, establishes the temperature at which thermal reactions take place within a sample, when it is heated continuously to an elevated temperature. The amount of divergence from base line is an indication of the differences in temperature between the sample and a reference substance such as thermally inert material like $\alpha\text{-Al}_2\text{O}_3$. DuPont 900 apparatus equipped with a high temperature cell was used for DTA. This equipment was provided with calibrated Platinum/Platinum-13 per cent Rhodium thermocouples under atmospheric conditions.

Thermogravimetry (TG) measures the loss in weight of the specimen under investigation with the increase in temperature at a predetermined rate. In this work Cahn thermogravimetric apparatus with a programmed temperature rise was used under atmospheric conditions. Dynamic method of obtaining dehydration curve was applied. Sample was heated at a rate of 10°C per minute and loss in the weight of the sample was recorded as a function of temperature. In DTG, rate of weight loss of the sample was plotted as a function of temperature i.e. $\text{dw}/\text{dt} = f(T)$.

Surface Area, Pore Volume and Pore Size Distribution:

Surface area of all the catalyst samples were measured by usual BET method. In this the amounts of nitrogen gas

adsorbed at different pressures, when the weighed sample was kept at liquid nitrogen temperature (-192°C approximately) after degassing it for complete removal of originally adsorbed water molecules, were measured. From such adsorption isotherms, surface area of the catalyst was calculated using BET equation. Pore volume and pore size were measured by mercury Winslow Porosimeter having range upto 15,000 psi.

Hydrocracking Reaction:

For carrying out this reaction a one liter high pressure autoclave (series 4000, Parr, Instrument Co., Moline, U.S.A.) was used as batch reactor. Detailed procedure and experimental set-up has been described by Choudhary [64]. However, a brief summary is given here.

The other parts of experimental set-up were (a) Annular furnace fitted with a rocking mechanism, (b) Reduced crude charging gun, (c) Hydrogen charging assembly, (d) Condensing coil immersed in a water bath, and (e) oil-gas separator. A schematic diagram of the assembly is given in Figure 3.2.

Known amount of catalyst (10 gms) was first of all taken in to the autoclave and was activated at a pressure of 10^{-2} torr and temperature of $20-30^{\circ}\text{C}$ higher than the operating temperature. Afterwards, weighed quantity of crude oil residuum (130 gms) was introduced in the autoclave with the help of charging gun and vacuum. Hydrogen was also charged upto the desired pressure. Heater was switched on along with the rocking

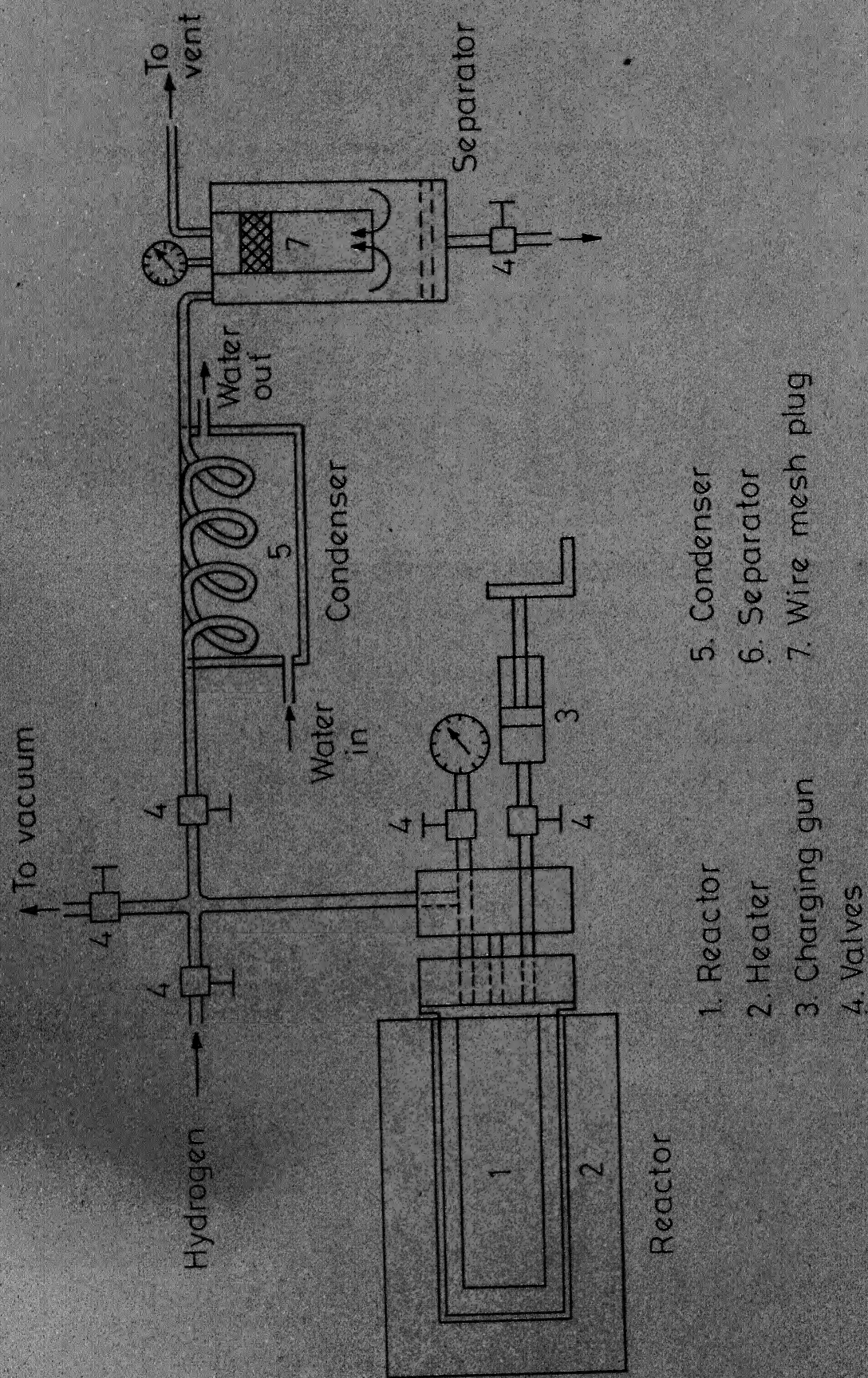


Fig 3.2- Schematic diagram.

system while reaction progressed. At the end of reaction time, oil-gas separator system was connected through the condenser and liquid product was collected in the lower part of the separator. Uncondensable gaseous product, mostly lower hydrocarbons, and hydrogen were vented into the atmosphere. The liquid product so obtained was fractioned and characterized.

CHAPTER 4

X-RAY ANALYSIS AND LEAST SQUARE REFINEMENT

4.1 Diffraction Phenomena:

X-rays are electromagnetic radiation having wave length approximately in the range of 0.5 - 2.5 Å. Monochromatic x-ray radiation can be obtained by using proper filter. When this monochromatic x-ray radiation encounters an atom, it is scattered. Coherent or unmodified scattering as well as incoherent or scattering of modified wavelength occurs. In crystals, atoms are arranged in a regular periodic fashion and coherently scattered x-rays from different atoms will have definite phase relationship and as they interfere in different directions, maxima and minima will occur. Thus diffraction is essentially, reinforced coherent scattering. The diffraction pattern obtained by scattering of x-rays by a crystal depends on its structure and arrangement of atoms. The angular positions of peaks or maxima are related to the shape and size of the unit cell, and their intensity to the positions of atoms. Any systematic absence in the diffraction maxima results from spacial symmetry and hence a systematic study of diffraction maxima gives information about crystallographic properties of the substance. Thus, using x-ray diffraction, one can determine the physical form of a catalyst in regard to its crystallinity. Positions of cations in

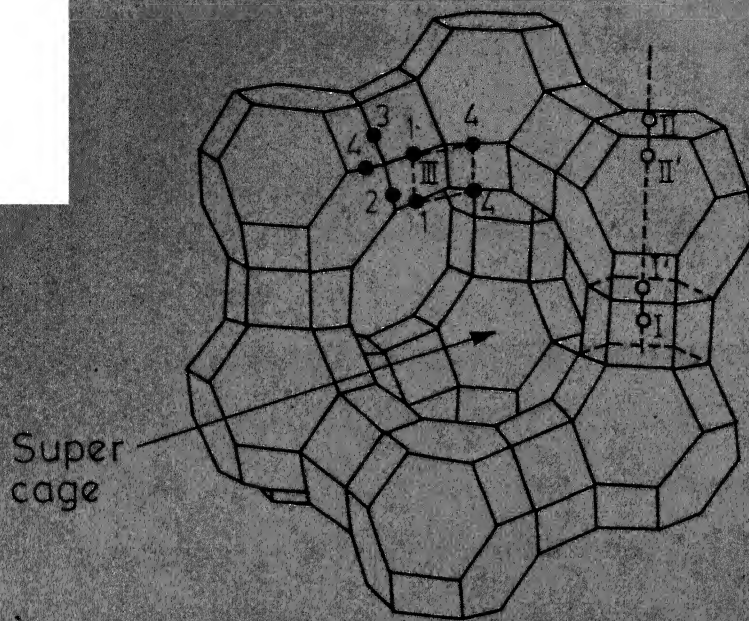


Fig. 4.3 - Faujasite framework and cation siting.

zeolite lattice is an important factor and greatly influences the catalytic activity and this information can be obtained by x-ray analysis. From this bond lengths and angles can also be calculated.

4.2 Aluminosilicate Framework Model and Site Nomenclature:

In Figure 4.1 is given idealized projection of sodalite unit with atom nomenclature and Figure 4.2 is section through abcdefghij in Figure 4.1 and shows relative positions of cation sites. These are reproduced from the work of Smith [30]. Same site nomenclature is used in this work. In Figure 4.3 is shown three dimensional model illustrating the super cage.

Basic model is that proposed by Shoemaker et al [31]. In this aluminosilicate framework model Si or Al are tetrahedrally coordinated by oxygen anions. These oxygen atoms are placed at the corner of near regular tetrahedra and center is occupied by either Al or Si atoms. Main building block for faujasite type structure is a octahedral group called sodalite due to its similarity with main structural unit of the mineral sodalite. Sodalite unit consists of 24 (Si,Al) ions interconnected with 36 oxygen anions. The shape of a sodalite unit is like a truncated octahedra and have 6 rectangular or (4-ringed) faces and 8 hexagonal faces (6 ringed). 24 vertices of a sodalite unit or beta cage are the centers of 24 tetrahedra and oxygen atoms lie near the mid point of edges, but are displaced to

attain the tetrahedral configuration around Si or Al (collectively called T atoms). In zeolite 13X, unit cell consists of eight sodalite units connected by double six-membered rings or hexagonal prisms and has point of symmetry T_d while zeolite A have O_h point of symmetry. T point group has four three fold axes, one being along each of the cubic body diagonals and two fold axes along each of the coordinate directions X, Y, and Z. T_d is a special case of T and has a diagonal mirror plane along one of the four three fold body diagonal axes [65]. This arrangement of sodalite units joined by the hexagonal prisms forms a very open framework with large cages in it. The large cages or super cages have a diameter of 16.34 \AA measured from centre to centre of two opposing oxygen atoms; they are interconnected by holes outlined by 12-membered $(Si, Al)_{12}O_{12}$ rings of about 10 \AA diameter. Supercage is connected to sodalite cage by a 'window' of 2.4 \AA . There are 8 sodalite cages, 8 supercages and 16 hexagonal prisms per unit cell.

Further classification of faces of truncated octahedron and frame work oxygen atoms are described below. There are four types of oxygen atoms, namely, O1, O2, O3 and O4 and they are located at different positions in the framework. Out of the 8 hexagonal rings of the sodalite unit 4 are shared by four connecting hexagonal prisms and the remaining 4 free hexagonal rings are shared with supercage. As shown in Figure 4.1 first type of hexagonal rings is formed by using O2 and O3 oxygen

atoms alternatively and the second type consists of O2 and O4 oxygens. 6 bridging 4-rings of octahedron are made of O3 and O4 oxygens. Hexagonal prism's 6 rectangular faces are composed of O1, O2 and O3.

4 axes of inverse 3-fold rotation symmetry intersect at site U (Figure 4.1), the centre of truncated octahedron. Extra-framework locations sites are also shown in Figure 4.1. Site I is a 16-fold site located at the centre of hexagonal prisms. It is chosen as original of the coordinate system. Site I' is a 32 fold site located in the sodalite cage and just outside the plane of a shared hexagonal face. Site II' is also a 32-fold site but is displaced from an unshared hexagonal face in to the sodalite cage. These are four I' and II' sites per sodalite unit. Site II is a 32-fold supercage site projecting slightly outwards from the free hexagonal face into the supercage. Site II* is displaced considerably into the supercage away from the 6-ring. Site V is located near the center of 12-membered ring between the supercages and have coordinates of $1/2, 1/2, 1/2$ (This site is not shown in the Figure 4.1). Site V is a 16-fold site and is situated at maximum distance from site I, which is the origin.

4.3 Calculation Procedures:

4.3.1 Unit Cell Constant and Interplaner Spacings: The interplaner distance (d_{hkl}), the measured angle of diffraction (2θ) and the wave length of the x-ray radiation (λ) used are

related by the well known Bragg's equation;

$$2d_{hkl} \sin \theta = \lambda \quad (4.1)$$

In the case of cubic system the relationship between the lattice parameter (a), miller indices (hkl), and interplanar spacing is given by

$$a = d_{hkl} \sqrt{h^2 + k^2 + l^2} \quad (4.2)$$

To get the best value of unit cell constant least square technique was applied.

Diffraction maxima i.e. peaks were assigned indices hkl using analytical or slide rule method [66]. Combining Eqs. 4.1 and 4.2 we get

$$\frac{\sin^2 \theta}{h^2 + k^2 + l^2} = \frac{\sin^2 \theta}{S} = \frac{\lambda^2}{4a^2} = \text{constant} \quad (4.3)$$

Since hkl are integers, the sum, $S = h^2 + k^2 + l^2$ is also an integer and $\lambda^2/4a^2$ is a constant for a given cubic crystal. Based on the above fact, indexing of cubic system can be done by finding a set of integers S which will yield a constant quotient when observed $\sin^2 \theta$ is divided by them, one by one. Once the proper integers S are found, the indices hkl of each line (diffraction maximum) can be written down from tabulated values available in the literature [67].

After getting the unit cell dimension for zeolite NaX-100, other informations like Al/unit cell, Si/Al ratio were obtained

from the plot of unit cell constant vs Al/unit cell given by Dempsey et al. [38].

4.3.2. Observed Structure Factor: From the relative intensity data, obtained by plotting number of counts at different points of the peaks and planimentering to get area under the peak, we can calculate observed structure factor by taking into account multiplicity factor, Lorentz polarization factor and scale factor. The relationship between structure factor (ratio of amplitude of wave scattered by unit cell to that of scattered by single electron) and relative integrated intensity is given by

$$I = S_q \{ F_o \}^2 P \left(\frac{1 + \cos^2 2\theta}{\sin^2 \theta \cos \theta} \right) \quad (4.4)$$

Since relative intensity I , the multiplicity factor P , scale factor S_q and Bragg angle 2θ are known for each line (diffraction maximum) on the pattern, we can find the magnitude of observed structure factor $|F_o|$ but we can not say anything about its phase. The term in the parenthesis in right hand side of Eq.4.4 is known as Lorentz-polarization factor.

Multiplicity factor, P , is defined as the number of different planes in a form. Since all these planes have the same spacing, the diffraction maxima corresponding to them will form part of the same cone and thus the intensity is observed in the same peak. The value of P for a class of planes hkl depends on the crystal symmetry. Values used in this work were taken from Cullity [66].

Lorentz polarization factor (LP) is a combination of two factors: (1) Polarization factor - It depends on the state of polarization of the incident x-ray and has the form of eq.4.4 for unpolarized beam. (2) Lorentz factor - This is the trigonometrical factor influencing the intensity and is due to the fact that practically observed peaks are not exactly at the Bragg's angle only, but it has certain width also. Therefore this correction is required. Values of L.P. correction factor used in this work were obtained from x-ray data book [67].

In powder method, one has to face one more difficulty. Reflections coincide in this analysis due to the various possible combination of miller indices (hkl) giving rise to same value of S or $h^2+k^2+l^2$. These combinations have different value of multiplicity factor and hence one has to distribute observed intensities among these set of possible planes. In this work, first of all, intensities were distributed in the ratio of multiplicity factor and then they were readjusted after each cycle of least square refinement so as to give better distribution among the set while total intensity of the set was kept constant.

4.3.3 Space Group Verification: The space group symmetry can be determined by identifying the systematically extinguished x-ray reflections. In our case reflections were present for the planes having all even or all odd miller indices (hkl). Not for all the planes having even miller indices, summation of hkl

was devisable by four (condition for diamond type cubic system) From International Table [68] space group satisfying these conditions was selected. It is $Fd\bar{3}m$ and stands for a face centered cubic system having inverse 3-fold diagonal mirror.

After knowing space group, one can easily find out what are the general positions, special positions and the equivalent points by consulting International Tables [68].

4.3.4 Structure Factor Calculation:

The structure factor $F(hkl)$ for a plane hkl is given by

$$F_{hkl} = \sum_{i=1}^N f_i a_i e^{2\pi i(hx_i + ky_i + lz_i)} \times e^{-T_i \frac{\sin^2 \theta}{\lambda^2}} \quad (4.5)$$

where N is the total number of atoms in a unit cell, f_i is atomic scattering factor and a_i is atom multiplier. T_i represents the isothermal temperature factor and x_i, y_i, z_i are fractional coordinates of atom i .

So if one knows the number of atoms in a unit cell, their coordinates, shape and size than the theoretical structure factor (F_c) can be calculated by using eqn. 4.5.

Atomic scattering factor f is reported as a function of $\sin \theta / \lambda$ [69]. It is the ratio of amplitude of the wave scattered by an atom to the amplitude of the wave scattered by one free electron. When $\sin \theta / \lambda = 0$ i.e. in case of forward

scattering, value of f is equal to atomic number of the atom concerned. In this work scattering factor for atom T(Si,Al) was calculated by averaging the scattering factor for Si^{4+} and Al^{3+} in the same ratio as they are present in the zeolite composition. Scattering factor for other atoms used were that for La^{3+} or N_i^{2+} , O^{2+} and Na^+ . These data are reported at an interval of $\sin\theta/\lambda = 0.1$, therefore, to get the data at a more close interval of $\sin\theta/\lambda = 0.05$, as required in the Least Square program (ORFLS) [70], method of interpolation was used after plotting the reported data.

For general position, atom multiplier, a_i is the ratio of number of atoms actually present at a particular site to the maximum possible equivalent positions for that site. When the site is fully occupied than its value is 1.0 other wise it is some fractional value. For special positions, one has to multiply the above mentioned ratio by the ratio of the special site's folds to the general site folds, to get the value of atom multiplier.

Isotropic temperature factor (T_i) was used to make correction for the thermal vibrations of the atoms. The atoms in a crystal oscillate around their mean positions due to thermal energy. The effect of this factor is reduction in observed intensity and consequently structure factors. Fractional coordinates x_i , y_i , z_i are obtained by dividing actual coordinates of the atom with unit cell constants a , b , and c

respectively. As in our case of cubic system $a=b=c$, all actual coordinates were divided only by unit cell constant a .

Starting value of coordinates and temperature factors were taken from earlier reported values [31,32],

4.3.5 Least Square Refinement:

In crystal structure analysis once a reasonable model of the detailed structure i.e. atomic coordinates is available, the next step is to improve these coordinates by some process of refinement. Least square is one of these refinement methods and is used most frequently in the final stage of structure determination, due to fast rate of convergence and absence of series termination error which are present in Fourier methods.

The necessary condition for a proposed model to be correct is that the values of calculated structure factor's should be as near to the observed structure factors as possible. Better the model, lesser will be the difference between calculated and observed values. To indicate the degree of closeness of the proposed structure to the actual crystal structure factors called reliability index R based on the square of structure factor F^2 or on the structure factor F itself, have been defined,

$$R = \frac{\sum |F_o^2 - (F_c)^2|}{\sum F_o^2} \quad (4.6)$$

$$R = \frac{\sum |F_o - F_c|}{\sum F_o} \quad (4.7)$$

A weighting scheme for observations may be used and then the above two relations take the forms

Weighted R based on F^2

$$R = \sqrt{W(F_O^2 - F_C^2)^2} / \sqrt{W(F_O^2)^2} \quad (4.8)$$

Weighted R based on F :

$$R = \sqrt{W(F_O - F_C)^2} / \sqrt{W F_O^2} \quad (4.9)$$

Here W is the weight used for particular observation.

In this work we used reliability factor based on F^2 and therefore values of R obtained were approximately double of that obtained for the same structure model but using conventional R based on F .

Least square refinement is based on the Legendre's principle which states that, when number of observations are more than number of variables to be determined then the most acceptable values of the variables are those which make the sum of squares of the errors a minimum. One would like to have as much experimental data as possible and then obtain the best solution by using least square technique. To make sum of the squares of the errors to be minimum their first derivative with respect to each variable is equated to zero. This gives rise to normal equations which will be same in number as the variables. These can be solved if the equations are linear. But relationship among structure factor and atoms coordinates is exponential

in nature. To get linear normal equations Taylor's expansion of the structure factor is used and first two terms are taken into account. Based on these consideration we obtain,

$$F = F_0 - F_c = \sum_j \left(\epsilon_{x_j} \frac{F_c}{x_j} + \epsilon_{y_j} \frac{F_c}{y_j} + \epsilon_{z_j} \frac{F_c}{z_j} \right) \quad (4.10)$$

here ϵ_{x_j} , ϵ_{y_j} and ϵ_{z_j} are errors in the positions coordinates of the j th atom, used for calculating F_c .

For each observed reflection, there exists an observational equation like (4.10) and by least squares method we can get normal equations.

To perform all these calculations, the full matrix least square program ORFLS [70] developed by Levy et al. was used. Listing of the program and special subroutines written for our case are given in Appendix B with input data required. Subroutine for matrix inversion in ORFLS was in FAP language and Dwivedi[71] converted this in the FORTRAN language. Starting values of coordinates and temperature factors were taken from the work of Shoemaker et al. [31] for the parent zeolite 13X and from Olson et al [32] for La-X samples. Temperature factors and occupancy factors were not varied simultaneously as these were highly correlated.

4.3.6 Bond Lengths and Angles:

When all the positions coordinates of the atoms in the crystal structure have been determined, it is of interest to

calculate the interatomic distances (bond lengths) and the angles between these distance vectors (bond angles). To calculate these distances and angles, general formula of coordinate geometry can be used. These calculations become some what complicated when the crystal system is not cubic and coordinates are not in ordinary orthogonal system. In such a case, one has to first convert them to orthogonal system [72] and then proceed with the calculations.

In general, for a Triclinic crystal systems, the square of interatomic distance between two atoms x_1, y_1, z_1 and x_2, y_2, z_2 is given by

$$\begin{aligned} S_{12}^2 = & (x_2 - x_1)^2 a^2 + (y_2 - y_1)^2 b^2 + (z_2 - z_1)^2 c^2 \\ & + 2(x_2 - x_1)(y_2 - y_1) ab \cos \gamma \\ & + 2(z_2 - z_1)(x_2 - x_1) ca \cos \beta \\ & + 2(y_2 - y_1)(z_2 - z_1) bc \cos \alpha \end{aligned} \quad (4.11)$$

Here α, β, γ are angles between three axes and a, b, c are unit cell constants of the triclinic system. Unit cell constants are introduced in the equation due to the fact that xyz are reduced co-ordinates.

As for cubic system $a=b=c$ and $\alpha=\beta=\gamma = 90^\circ$, above equation is simplified to

$$S_{12}^2 = a^2[(x_2 - x_1)^2 + (y_2 - y_1)^2 + (z_2 - z_1)^2] \quad (4.12)$$

Relationship for calculating bond angle between two vectors \vec{S}_{12} and \vec{S}_{13} meeting at point x, y, z , is given by

$$\cos \psi = \frac{\bar{S}_{12} \cdot \bar{S}_{13}}{S_{12} S_{13}} \quad (4.13)$$

In the above equation the numerator is scalar product of two vectors and the denominator is simply the arithmetic product of the lengths of the two vectors.

For calculation of the numerator in a general trielinic system, formula used is

$$\begin{aligned} \bar{S}_{12} \cdot \bar{S}_{13} = & (x_2 - x_1)(x_3 - x_1)a^2 + (y_2 - y_1)(y_3 - y_1)b^2 \\ & + (z_2 - z_1)(z_3 - z_1)c^2 + [(x_2 - x_1)(y_3 - y_1) \\ & + (y_2 - y_1)(x_3 - x_1)]ab \cos \gamma \\ & + [(z_2 - z_1)(x_3 - x_1) + (x_2 - x_1)(z_3 - z_1)]ca \cos \beta \\ & + [(y_2 - y_1)(z_3 - z_1) + (z_2 - z_1)(y_3 - y_1)]bc \cos \alpha \end{aligned} \quad (4.14)$$

For cubic system this reduces to

$$\bar{S}_{12} \cdot \bar{S}_{13} = a^2[(x_2 - x_1)(x_3 - x_1) + (y_2 - y_1)(y_3 - y_1) + (z_2 - z_1)(z_3 - z_1)] \quad (4.15)$$

Based on above formula, a computer program was developed by Dwivedi [71] which can be used for Triclinic, monoclinic, orthorhombic, tetragonal and cubic unit cells. This program also calculates standard deviations (s.d.) in bond lengths and bond angles if s.d. in coordinates are provided. For calculation of s.d., expressions given by Darlow [73] were used. Listing of the program and input data required are reported in Appendix B.

CHAPTER 5

RESULTS AND DISCUSSION

5.1 Ion Exchange: Unit cell compositions of lanthanum and nickel exchanged zeolites, calculated from flame photometric analysis, are given in Table 5.1. Table 5.2 contains detailed information on degree of lanthanum exchange as a function of time and number of equilibrations. Coordinates of the exchange isotherm for LaX-79 and LaX-96, defined by Sherry [21] as the equivalent fraction of La^{3+} ions in zeolite phase (Y coordinate Z_{La}) and equivalent fraction of La^{3+} ions in solution phase (X-coordinate S_{La}) are also included in Table 5.2. On careful scrutiny of these results one can reach at the following conclusions:

1. Degree of exchange depends on the number of days for which it is allowed to continue. But the increment in the degree of exchange is not proportional to the increment in number of days. Major contribution in extent of exchange is from first equilibration, while the share of the subsequent exchanges keep on diminishing. From these facts it is obvious that the exchange reaction becomes increasingly difficult, as the concentration of the residual sodium ions in the zeolite lattice diminishes. This can be explained in terms of sodium atoms occupying different types of sites. Mobile sodium ions and those located at site II can be exchanged more easily compared to those situated at site I. As the radius of the hydrated

TABLE 5.1: CHEMICAL COMPOSITION OF ZEOLITE CATALYSTS

Properties Catalyst	Degree of Exchange, Per cent	Unit Cell Composition, Number of			DTA	DTA
		Cations ^a		H ₂ O ^c	Endotherm Tempera- ture, °C	Exotherm Tempera- ture, °C
		Na ⁺	M ^{n+b}			
NaX-100	100	86	0	215	-	-
LaX-58	58	36.2	16.6	226	599,664	> 780
LaX-79	79	18.2	22.6	260 ^d	568,612	> 780
LaX-96	96	3.5	27.5	240	204	> 780
NiX-80	80	17.2	34.4	285	-	-

^aCalculated from flame photometric analysis

^bMetal cation exchanged

^cCalculated from TG results on the basis of anhydrous mass at 800°C

^dIn the form of powder made from pellets

TABLE 5.2: LANTHANUM ION-EXCHANGE RESULTS

Catalyst	Equilibrium Batch	No. of days of equilibration	Concn. of Na ⁺ in the filtrate of the batch	Isotherm Coordinates		Degree of Exchange
				S_{La}	Z_{La}	
LaX-79	NIK-121	3	800	0.826	0.620	61.5
	NIK-122	5	120	0.974	0.714	8.5
	NIK-123	4	20	0.996	0.728	1.5
	NIK-124	2	92 ^a	0.970	0.799	6.5
	NIK-125	2	13	0.997	0.809	1.0
<hr/>						
LaX-96--	NIK-131	5	900	-	-	69.5
	NIK-132	4	204	-	-	15.5
	NIK-133	25	144 ^a	-	-	11.0

^aThe zeolite sample was given heat treatment before starting this batch equilibrations.

La^{3+} ions (3.96 \AA) is greater than the size of aperture (2.4 \AA) connecting sodalite cage with supercage, it can not reach site I unless water associated with it is stripped off by heating and radius is reduced to its ionic radius (1.15 \AA). Similar type of results and explanations have been reported by many workers [16, 17, 29, 44].

2. The increased concentration of sodium ions in the filtrate batches NIK-124 and NIK-133 (Table 5.2) indicates that intermediate heat treatment of partially exchanged zeolite is helpful in accelerating the residual ion exchange. Intermediate heating causes the migration of exchanged cations, located in the channels and associated with water molecules, to Site I. This migration results in sodium ions displacement from Site I to more accessible sites [29, 44]. Due to this treatment higher degree of exchange (96 per cent) was achieved even at a lower temperature (70°C) compared to the those reported by Sherry [21] (92 per cent exchange at 82°C).

3. By examining the values of exchange isotherms coordinates (Table 5.2) one can conclude that lanthanum ions prefer solution phase (higher value of S_{La}) compared to the zeolite phase (lower value of Z_{La}). This is due to the use of concentrated salt solution. The selectivity of higher charged ions (La^{3+}) in zeolite phase can be increased by employing a very dilute solution [21].

5.2 Differential Thermal Analysis (DTA) and Thermogravimetry (TG):

For all the catalysts studied, plots of weight loss with rise in temperature i.e. thermogravimetric curves are shown in Figure 5.1. To get the information about different types of intrazeolitic water binding, differential thermogravimetric (DTG) curves were obtained by plotting inverse of water loss rate ($\Delta T / \Delta W$) as a function of temperature (T) (Figure 5.2). The number of water molecules per unit cell for different samples, as determined from TG measurements, are listed in Table 5.1. Their plot against degree of La^{3+} exchange is shown in Fig. 5.3. Figure 5.4 contains differential thermal analysis curves for lanthanum exchanged zeolite samples.

From the data on water molecules per unit cell (Table 5.1 and Figure 5.3) we make the following observations.

In Table 5.1 is shown that NiX-80 sample contains about 10 per cent more water molecules than LaX-79 (in powder form). By examining the TG curves for NiX-80 and LaX-79 (Figure 5.1) it also becomes clear that for NiX-80, not only the total weight loss is more than that for LaX-79, but it also remains higher throughout the range of heating. One cannot explain the differences in water content of the zeolite samples, having different cations but same degree of exchange, simply on the basis of number of cations per unit cell i.e. cation density. Cation density consideration leads to a conclusion that NiX-80

LIBRARY
CENTRAL LIBRARY
KNOX

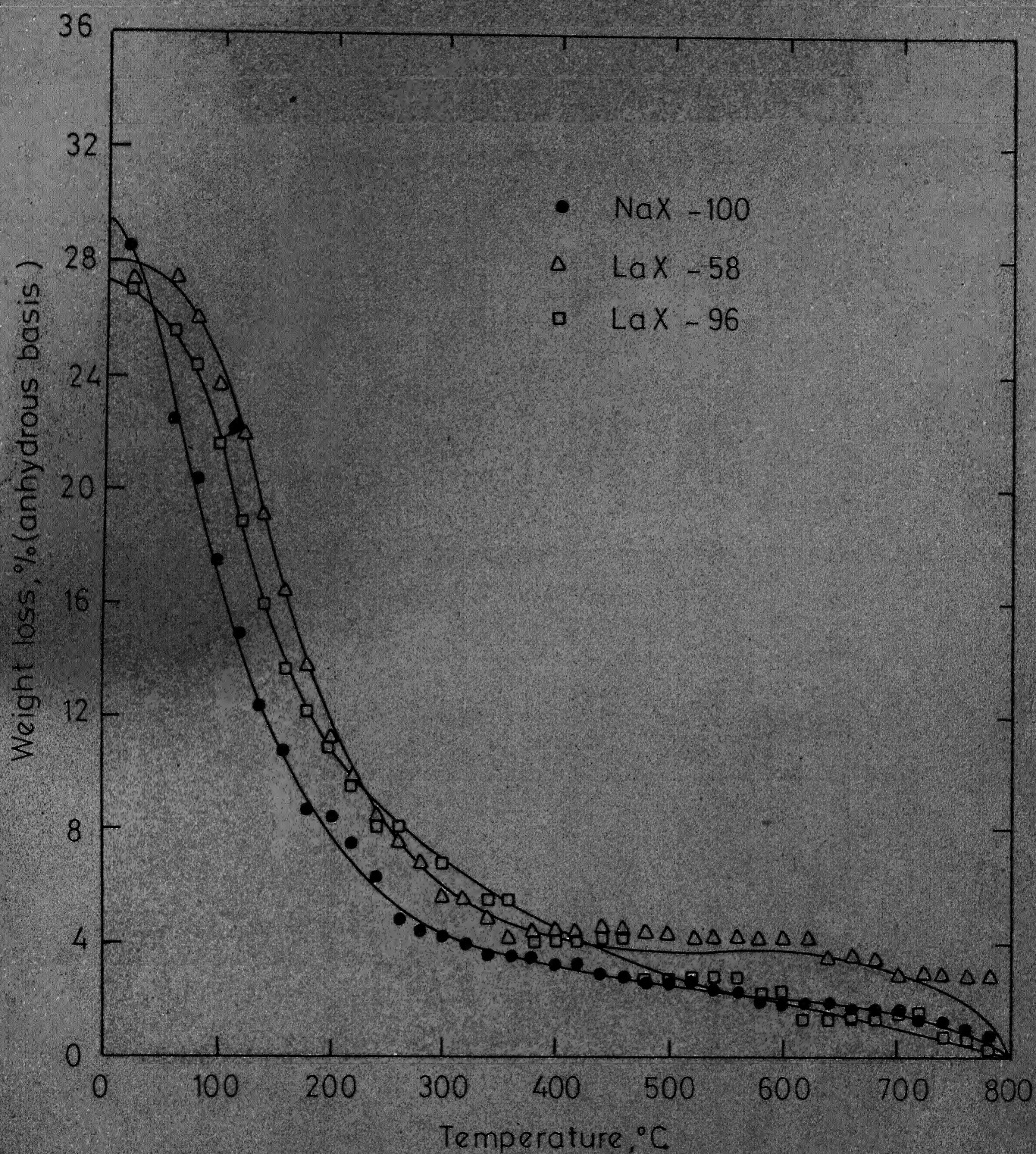


Fig. 5.1 - Thermogravimetric curves for NaX-100, LaX-58 and LaX-96 catalysts.

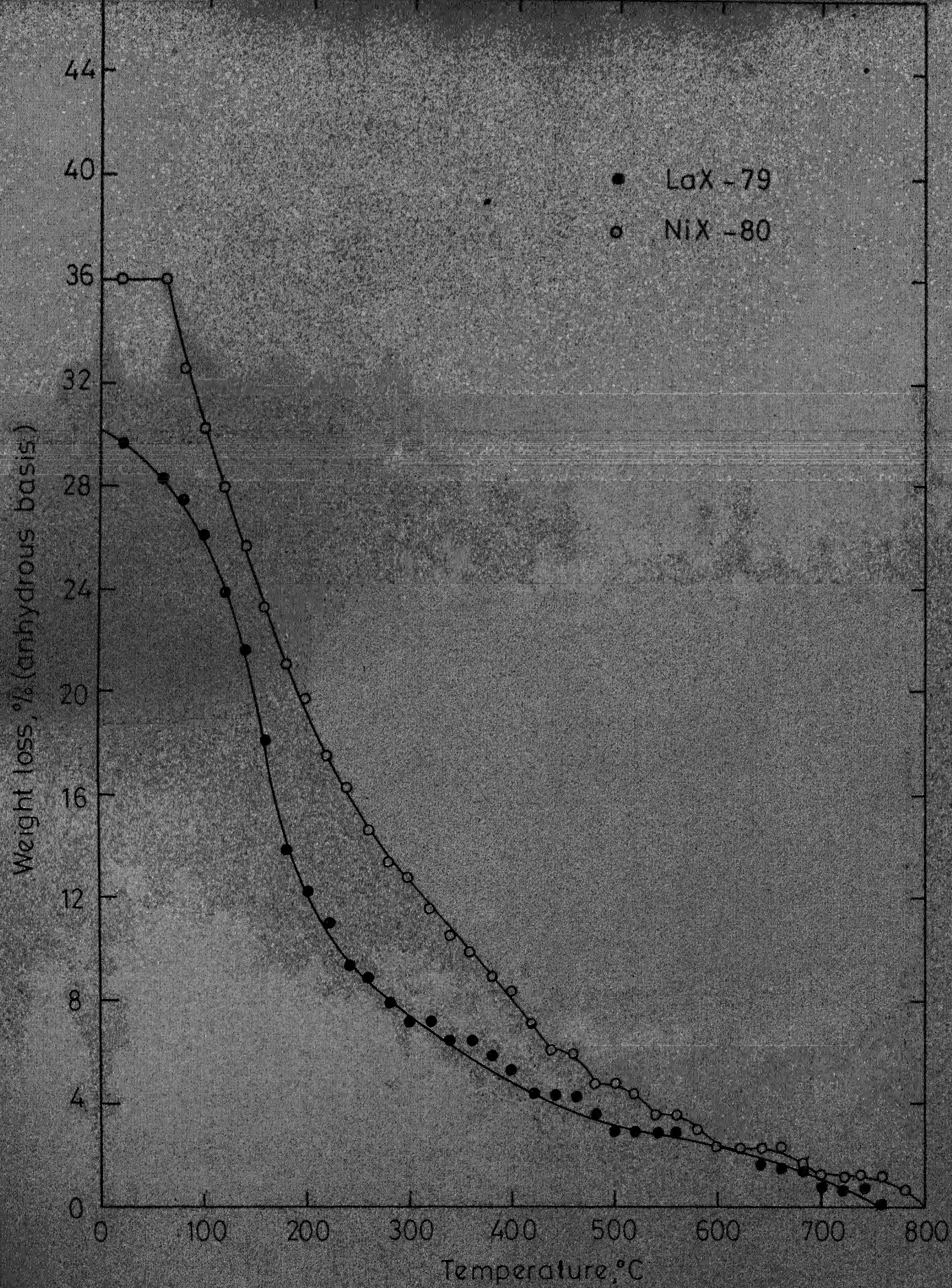


Fig. 5.1 - Thermogravimetric curves for LaX-79 and NiX-80 silica-alumina catalysts.

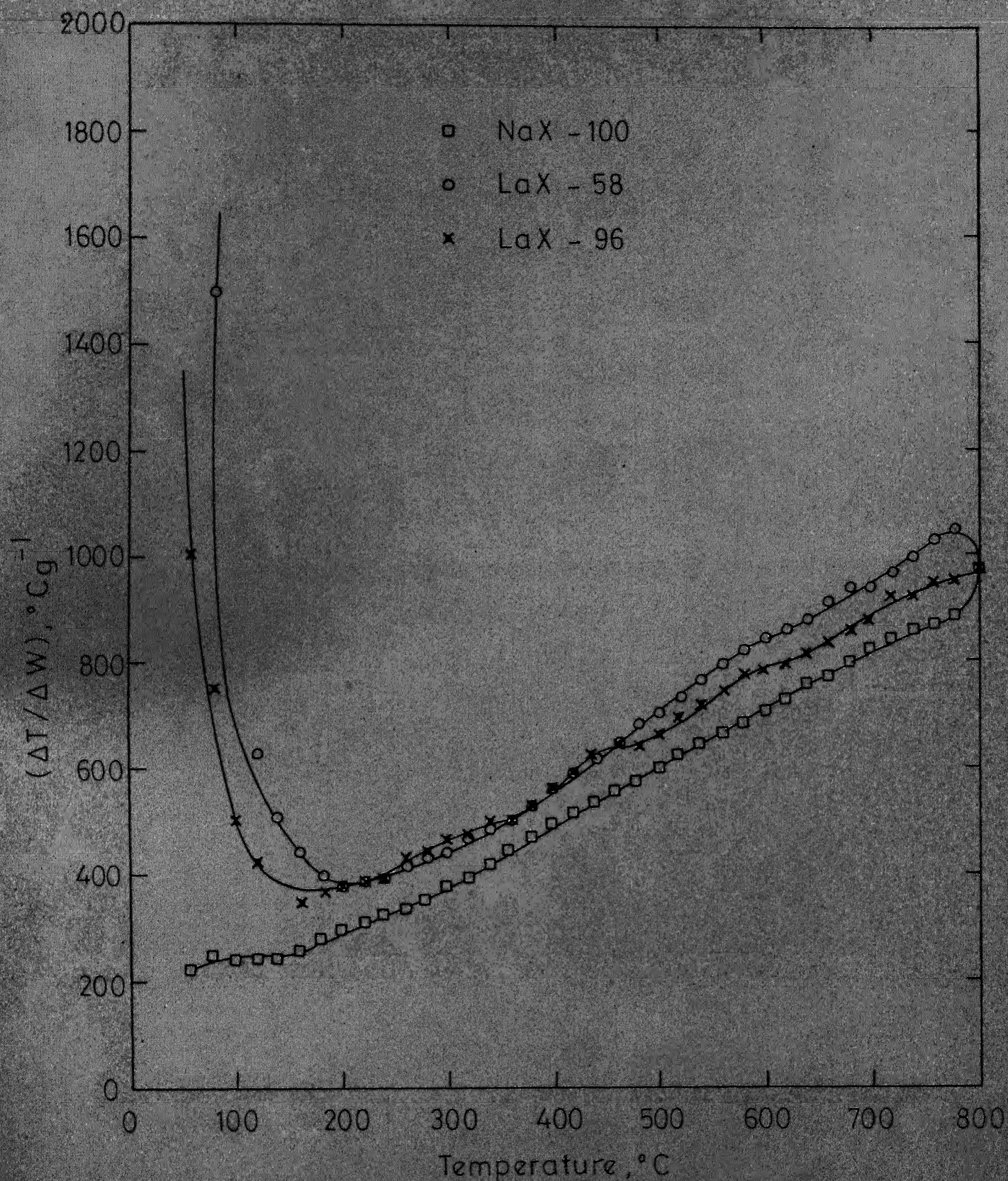


Fig. 5.2- Differential thermogravimetric curve for NaX-100, LaX-58 and LaX-96 catalysts.

Contd...

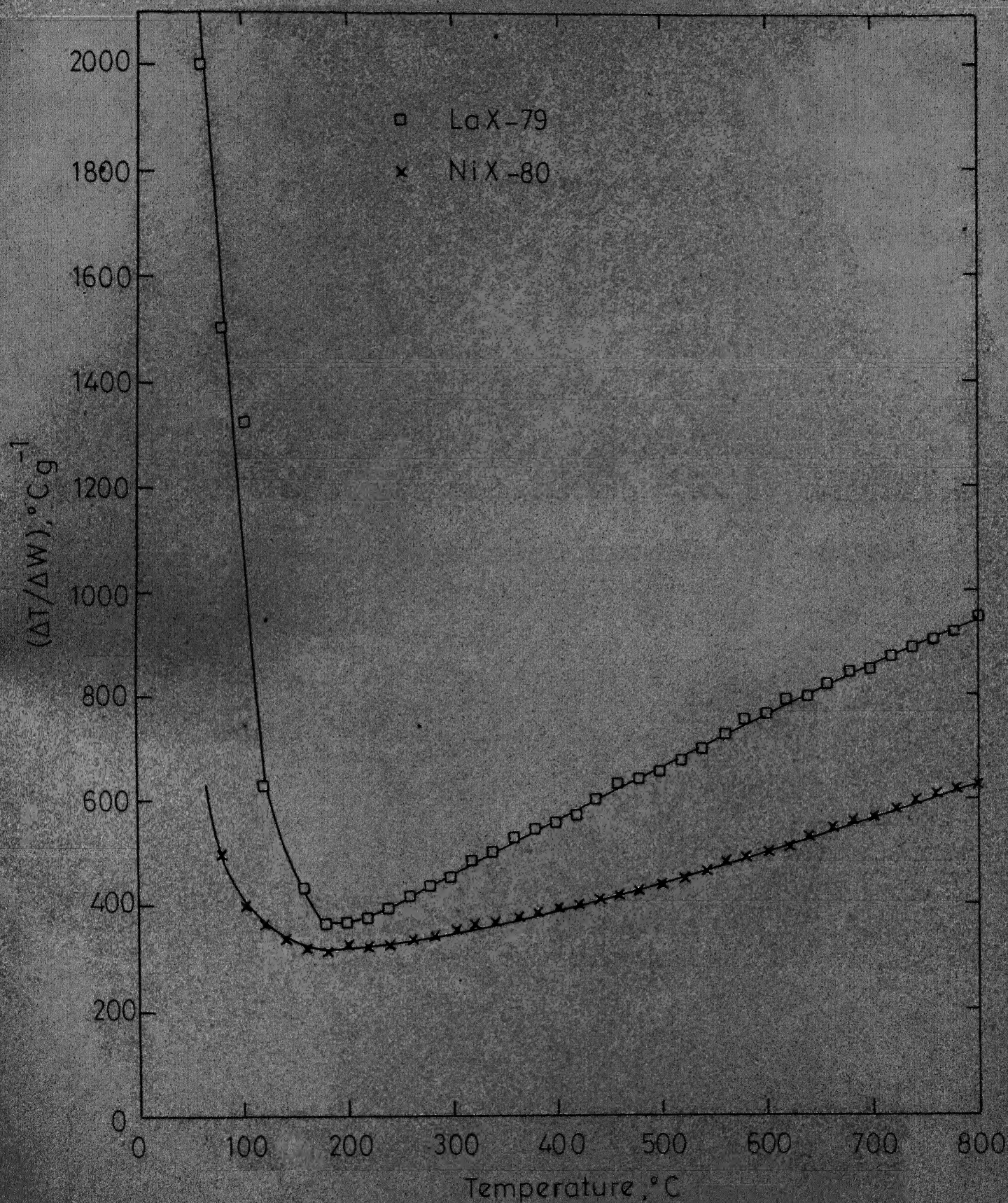


Fig 5.2 - Differential thermogravimetric curves for LaX-79, NiX-80 and silica alumina catalysts.

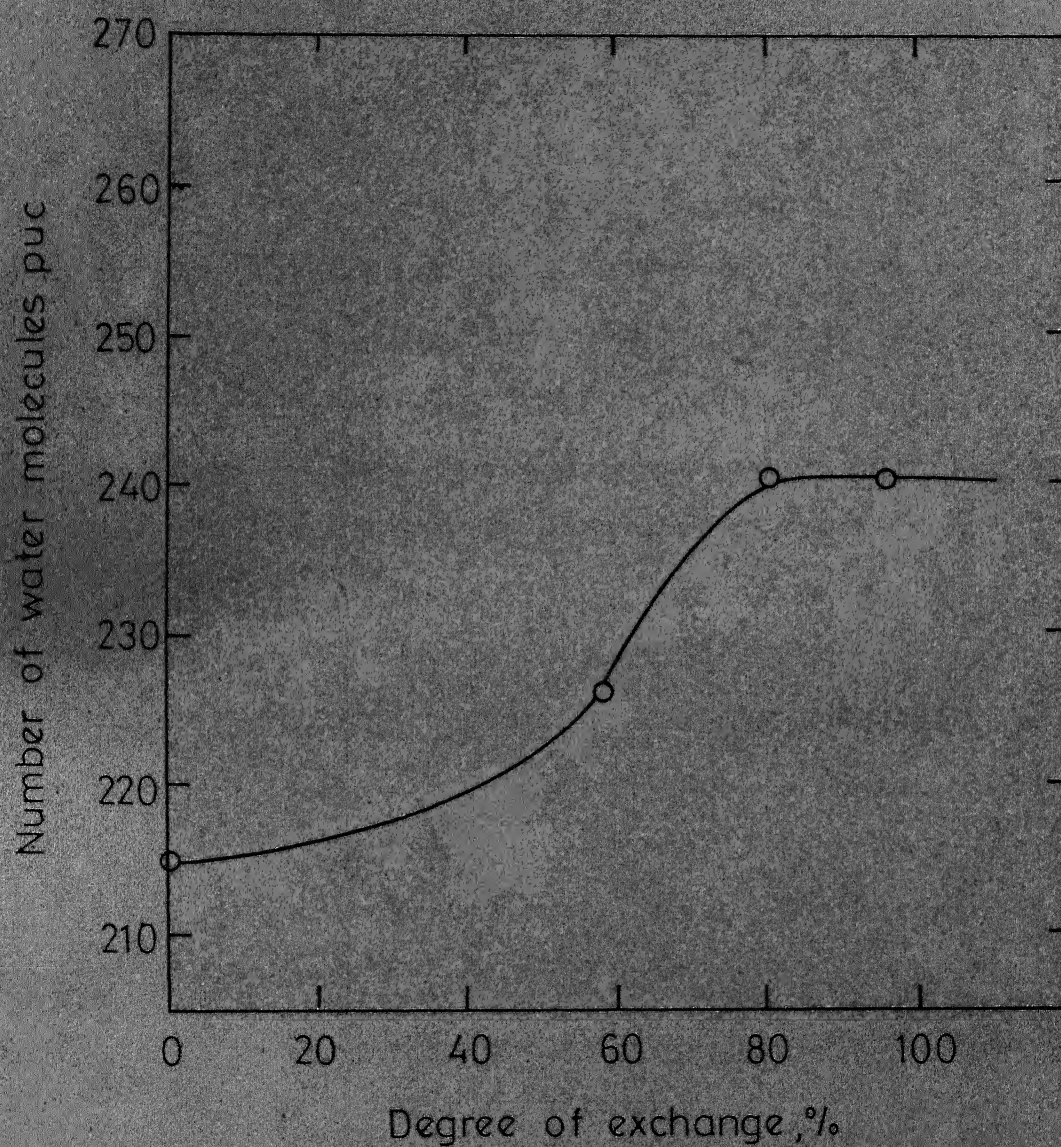


Fig. 5.3 - Variation in the number of water molecules with the degree of exchange.

having 34.4 Ni^{2+} ions should contain less water molecules than LaX-79, which have only 22.6 La^{3+} ions. But when one also considers the smaller size of Ni^{2+} ions (0.72 \AA) compared to that of La^{3+} (1.15 \AA), then it is easy to see that there is more free space available for water molecules in the former case and therefore higher water content can be expected.

From Figure 5.3 one observes that number of water molecules per unit cell increases with increase in degree of lanthanum exchange upto 82 per cent, beyond which no perceptible increase is noticed. Coughlar and Carroll [74] have also reported similar finding. This levelling of water content may be due to overcrowding of supercage after 82 per cent exchange level and there is no space available for more water molecules. It will be shown in section 5.5 during discussion of x-ray analysis results that total number of La^{3+} ions, which could be located by least square refinement of LaX-96 is less than that in LaX-79. This indicates that after certain degree of exchange (around 82 per cent) La^{3+} ions become mobile and come out to the supercages and thus cause overcrowding.

DTA curves for LaX samples (Fig. 5.4) indicate a continuous loss of water over a broad range of temperature. Two endotherms are shown by each of the LaX samples. The low temperature DTA endotherm is (at about 200°C) pertains to the dehydration of the zeolite i.e. removal of free water molecules. The high temperature endotherm (at about 600°C) is due to the loss of

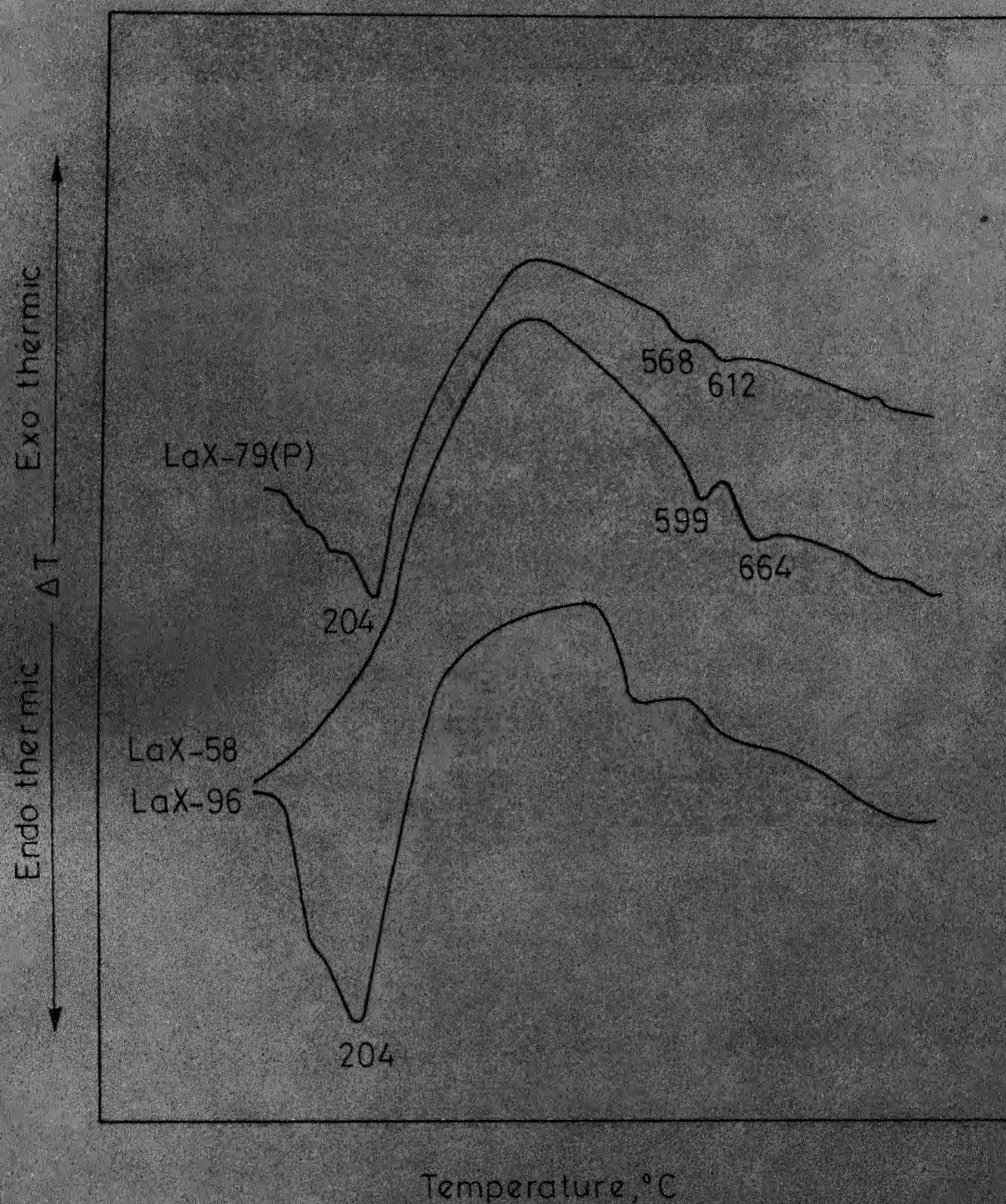


Fig 5.4 - Trace of DTA thermograms for LaX-58, LaX-79 and LaX-96 catalysts.

Water from hydroxylated cations (removal of more rigidly bound water molecules). Breck [16] has also reported the existence of these additional endotherms at for polyvalent exchanged zeolites and has explained their presence in terms of hydration complexes formed by polyvalent cations.

5.3 Surface Area, Pore Volume and Pore Size Distribution:

These results for all the catalysts are presented in Table 5.3 along with true density and apparent density data. NiX-80 sample showed much smaller area compared to those of parent NaX-100 or LaX catalysts. This decrease in surface area can be explained in terms of partial loss of crystalline structure also shown by x-ray analysis results, [Section 5.5]. Surface area seems to decrease with increasing degree of lanthanum exchange. Pore size distribution data indicate that smaller pores ($4-60\text{\AA}$) are in large number (about 60 per cent) in case of NiX-80, whereas NaX or LaX catalyst have only 20 to 30 per cent in this range. The pore volume is reduced by ion-exchanging Na^+ with Ni^{2+} or La^{3+} ions.

5.4 Hydrocracking :

The effect of degree of exchange on the percentage conversion, defined as the weight per cent of feed stock converted to liquid products having a maximum boiling temperature as the reaction temperature, is shown in Figure 5.5. In this figure a comparison of the performance of LaX catalysts having three different degrees of exchange, namely, 58, 79, and 96 percent

TABLE 5.3: SURFACE AREA, PORE VOLUME AND PORE SIZE DISTRIBUTION DATA

Catalyst	True density gm/cc (by He)	Apparent density gm/cc (by Hg)	Pore Volume cc/gm	Surface area m ² /gm	Pore Size Distribution (per cent by Volume)									
					4-60 Å	60-100 Å	100-200 Å	200-300 Å	300-400 Å	400-500 Å	500 - 75000 Å			
NaX-100	0.3627	0.7550	0.3923	450.01	29.2	3.2	4.2	3.2	2.1	2.1	2.1	56.0		
NaX-58	0.3365	0.7035	0.3670	454.8	23.8	3.2	4.9	3.3	2.2	2.2	2.3	60.3		
LaX-79	0.3686	0.9212	0.5526	348.2	20.3	3.2	2.6	1.7	1.7	1.7	1.6	68.9		
LaX-96	0.3208	0.6827	0.3619	326.9	31.7	2.4	3.0	3.7	2.0	2.0	1.4	55.8		
NiX-80	0.3666	0.6852	0.3186	217.0	57.7	5.10	6.1	3.7	2.5	2.5	2.9	22.0		

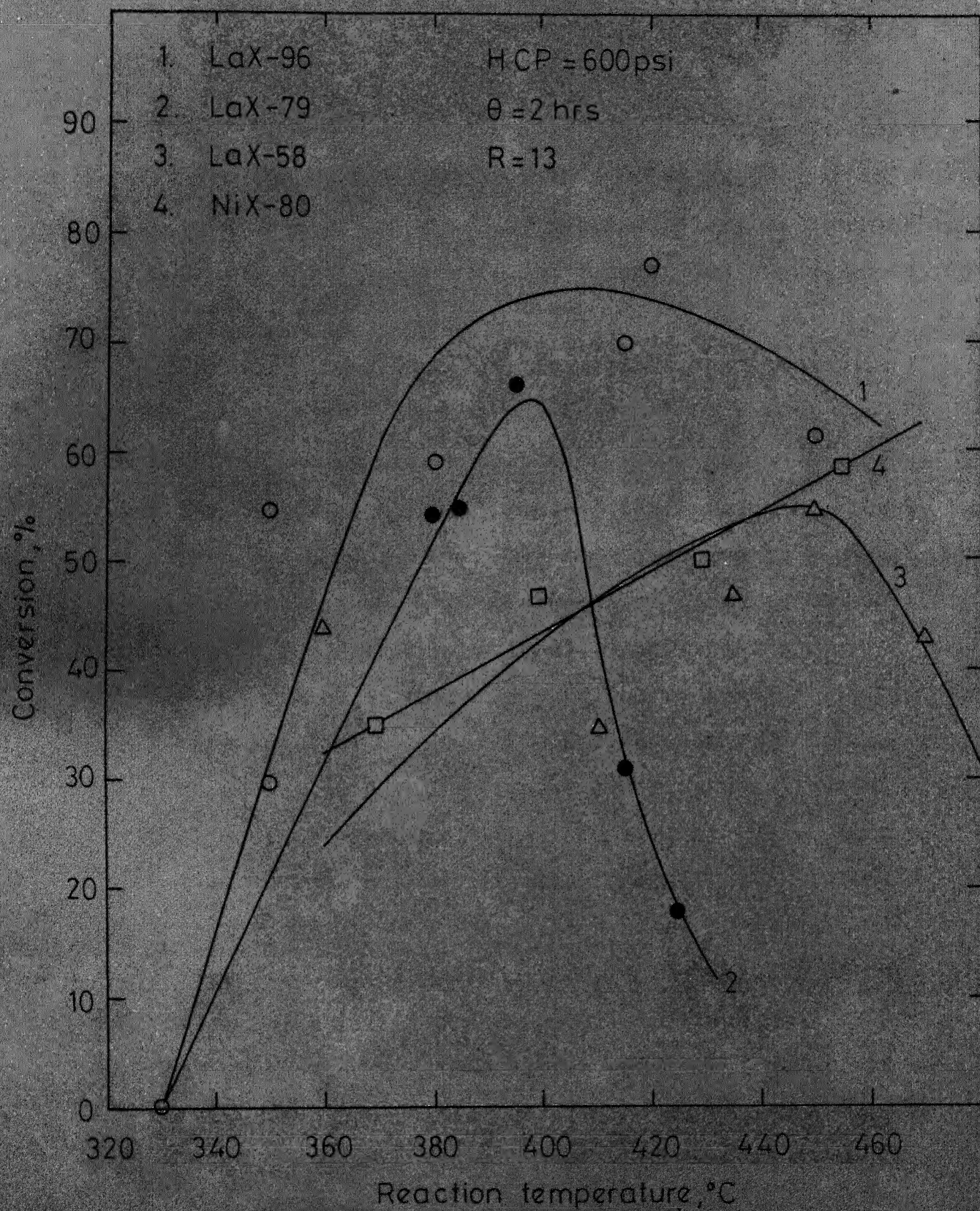


Fig. 5.5-A comparison of the performance of different catalysts

is made. To see the effect of nature of cation, the conversion curve for NiX-80 catalyst is also plotted on the same figure. All these data are at constant hydrogen charging pressure (HCP) of 600 psi, reaction time (θ) of 2 hours and charge to catalyst ratio (R) of 13.

By studying Figure 5.5 one notices that to attain a given conversion, temperature required is lower in the case of catalyst having higher degree of exchange. So catalytic activity of the catalyst increases with increase in degree of exchange. Otouma et al [75] have also reported similar results. The increase in the degree of exchange causes an increase in the number of acid sites and their strength. Higher the degree of exchange more acidic is the catalyst. This type of close relationship between acidity of catalyst and its activity is valid for the cracking reactions where thermal mode of cracking is not significant [76]. In present work also thermal mode of cracking can not be contributing much as the operating temperature was not very high.

The location of cations affects the acidity of the catalysts. If cations are situated at site I then there is no observable rise in its acidity. When cations occupy site I' or II i.e. more accessible sites than the increase is very significant. In this study as the catalysts in the autoclave cannot be dehydrated completely and some residual water molecules are always present so the lanthanum cations should

be occupying site I' and II only. Same result was obtained by our structure refinement study (presented in section 5.5). It was also found in the above study that after certain degree (around 80 per cent) exchange, La^{3+} ions become mobile and come out from interior sites to the supercages, and thus being more accessible, they cause significant increase in acidity and hence catalytic activity.

The lower activity of the Ni^{2+} exchanged zeolite is due to the partial loss of structure as is also reported by many other workers [44, 45, 46, 47]. This fact was also supported by our surface area and x-ray analysis results.

5.5 X-ray Analysis and Structure Refinement:

The values of lattice parameters (a) for each sample are presented in Table 5.4 and are in good agreement with reported data [77]. Si/Al ratio for parent zeolite was found to be 1.23, the presence of 86 aluminum atoms per unit cell was confirmed by using the plot given by Dampsey et al. [38]. The interplanar spacings, the indices (hkl) of various reflection and their relative intensities for different zeolite samples are presented in Appendix A. For the purpose of comparison published data [16] for NaX-100 sample is also included in the Table A.2. Appendix A also contains the values of square of observed and calculated structure factors obtained from the last cycle of the least square refinement. Final atomic parameters, reliability indices, occupancy factors, and temperature factors are given in Table 5.5. Table 5.6 contains

TABLE 5.4: UNIT CELL PARAMETER OF ZEOLITE CATALYSTS

Catalysts	Degree of Exchange per cent	Unit Cell parameter \AA
NaX-100 (Si/Al=1.25)	100	24.93 [13]
NaX-100 (Si/Al=1.23)	100	24.9954
LaX-58	58	25.0215
LaX-79	79	25.0252
LaX-96	96	25.0243
NiX-80	80	25.0197

TABLE 5.5: FINAL ATOMIC PARAMETERS
(Origin at $\bar{3}$ m)

Catalyst	Atom	Positions	Occupancy factors	Parameters			Temperature factor (\AA^2)
				x (\AA)	y (\AA)	z (\AA)	
1	2	3	4	5	6	7	8
NaX-100	T(Si,Al)	192(i)	1.0	-0.03925	0.14296	0.02857	4.70
	01	96(h)	1.0	-0.10695	0.10695	0.00000	7.00
	02	96(g)	1.0	-0.01484	0.09492	-0.01484	10.90
	03	96(g)	1.0	-0.01086	0.07424	0.07424	3.46
	04	96(g)	1.0	-0.05278	0.16493	0.08507	8.84
R=0.250 Na ⁺ ions located $\equiv 4B$	Na ₁	16(c)	1.0	0.0	0.0	0.0	5.00
	Na ₂	32(e)	1.0	0.24129	0.24129	0.24129	5.60
LaX-96	T(Si,Al)	192(i)	1.0	-0.03222	0.15834	0.02492	4.70
	01	96(h)	1.0	-0.09363	0.09363	0.0	7.00
	02	96(g)	1.0	0.01234	0.10452	0.01234	10.90
	03	96(g)	1.0	0.03691	0.08462	0.08462	3.46
	04	96(g)	1.0	-0.04031	0.16662	0.03338	8.84
	1A2	32(e)	0.16	0.10092	0.10092	0.10092	3.74
	0W3	32(e)	1.0	0.16153	0.16153	0.16153	6.00
							5

Table 5.5 (contd)

1	2	3	4	5	6	7	8
R=0.228	IA4	32(e)	0.25	0.25267	0.25267	0.25267	5.94
Total La ³⁺							
ions lo-	LA5	16(d)	0.00	0.5	0.5	0.5	6.00
cated							
=13.12							
LaX-79	T(Si,Al)	192(i)	1.00	-0.05324	0.15461	0.01940	4.70
	01	96(h)	1.00	-0.11325	0.11325	0.0	7.00
	02	96(g)	1.00	0.03770	0.11688	0.03770	10.90
	03	96(g)	1.00	0.00719	0.06000	0.06000	3.46
	04	96(g)	1.00	-0.03159	0.15660	0.09340	8.84
	LA2	32(e)	0.32	0.07045	0.07045	0.07045	3.74
R=0.165							
Total La ³⁺	IA4	32(e)	0.51	0.24879	0.24879	0.24879	5.94
ions lo-	OW3	32(e)	1.00	0.14961	0.14961	0.14961	6.00
cated							
=25.56	LA5	16(d)	0.00	0.5	0.5	0.5	6.00
LaX-58	T(Si,Al)	192(i)	1.0	-0.06323	0.14112	0.05565	4.70
	01	96(h)	1.0	-0.11025	0.11025	0.0	7.00
	02	96(g)	1.0	0.00369	0.09960	0.00369	10.90
	03	96(g)	1.0	-0.01835	0.05881	0.05881	3.46
	04	96(g)	1.0	-0.02687	0.16064	0.08936	8.84
	Na1	16(c)	1.0	0.0	0.0	0.0	5.00

Table 5.5 (contd)

1	2	3	4	5	6	7	8
	Na ₂	32(e)	0.68	0.193101	0.193101	0.193101	5.60
	LA2	32(e)	0.0	0.06920	0.069200	0.06920	3.74
R=0.272	OW3	32(e)	1.0	0.20546	0.20546	0.20546	6.00
Total La ³⁺ =	LA4	32(e)	0.49	0.24220	0.24220	0.24220	5.71
ions located =15.68	LA5	16(d)	0.0	0.5	0.5	0.5	6.00
Na ⁺ ions located =37.76							

TABLE 5.6: INTER ATOMIC DISTANCES AND ANGLES FOR
DIFFERENT ZEOLITE SAMPLES

A	Atom Set	NaX-100	LaX-58	LaX-79	LaX-96
Distances (Å)	T-01	2.05	1.97	1.89	2.32
	T-02	1.73	2.37	2.51	1.76
	T-03	2.18	2.35	2.98	2.94
	T-04	1.55	1.34	1.93	1.50
	01-02	2.35	2.87	3.90	2.69
	01-03	3.14	3.02	3.62	3.89
	01-04	2.91	3.31	3.29	3.05
	02-03	2.29	1.80	1.71	1.97
	02-04	3.19	2.74	2.44	2.72
	03-04	2.51	2.67	2.74	2.87
	Na1-01	3.78	-	-	-
	Na1-03	2.64	-	-	-
	Na2-02	3.75	-	-	-
	Na2-04	3.11	-	-	-
Angles (Degrees)	01-T-02	76.55	82.02	124.31	81.48
	01-T-03	96.05	88.03	93.24	95.06
	001-T-04	107.04	172.70	118.97	103.77
	02-T-03	70.54	44.86	34.87	40.66
	02-T-04	153.28	90.86	65.13	112.78
	03-T-04	82.74	88.04	63.39	72.36
	T-01-T	148.20	163.87	159.76	177.18
	T-03-T	135.93	79.98	106.43	107.03
	T-04-T	126.60	89.14	88.32	103.58
	T-02-T	69.15	49.17	82.06	92.21

TABLE 5.7: AVERAGE BOND LENGTHS (\AA) AND ANGLES($^{\circ}$)
FOR THE FRAMEWORK OF ZEOLITE SAMPLES

Distances (\AA)	Atom set	NaX-100	LaX-58	LaX-79	LaX-96
	T-O	1.88	2.00	2.32	2.23
	O-O	2.73	2.74	2.95	2.86
Angles (Degrees)	O-T-O	97.70	94.41	83.31	86.02
	T-O-T	119.97	95.53	109.14	120.00

bond lengths and angles, calculated from final atomic parameters, and their average values are given in Table 5.7.

As is shown in Table 5.4 the replacement of sodium ions causes an increase in the lattice parameter, both in the case of nickel and lanthanum exchanged zeolites. In the latter case the increase is noticed only upto 79 per cent exchanged level after which there is a slight decrease. The intensity data were also affected by the degree of La^{3+} exchange (Appendix A). In the zeolites samples, having higher level of exchange, the intensities of lower angle peaks decreased while those of medium angle peaks increased. Some higher angle peaks which were absent in NaX-100 were also observed in La^{3+} exchanged samples like LaX-79 and LaX-58. But these higher angle peaks were very weak in intensity and their absence in original sample can be attributed to low sensitivity of the diffractometer (XRD-5) used for its recording. The changes in intensity data can be explained in terms of different site selectivity of La^{3+} ion compared to that of sodium ions [31,32,50].

The most drastic change in peak intensities was observed in the case of NiX-80 sample. Intensities of almost all the peaks were reduced and some of the peaks were virtually missing. Also the background intensity was too high. This reduction in intensity can be due to distortion of framework tetrahedra and disorder in the structure, which shows up as high temperature factor for nickel exchanged samples. The

high temperature factors would result from enhanced thermal vibration which would indicate less stable zeolite structure. It has been suggested by many workers [44, 45, 46, 47] that Ni^{2+} exchanged zeolite X sample, upon calcination, partially loses its crystal structure. Serpinski et al. [47] have reported decrease in the propane adsorption capacity with increase in degree of nickel exchange in the zeolite X. As the number of reflections observed were small in the case of NiX-80 sample, the least square refinement was not attempted.

By carefully examining the occupancy factors of La^{3+} ions in different samples [Table 5.5] one can arrive at some very important conclusions.

First of all we see that upto 58 per cent exchange, nearly 38 Na^+ ions occupy sites I and II (16 Na^+ ions at site I and 22 at site II). No sodium ion of site I is removed upto this level of exchange. Out of nearly 48 Na^+ ions replaced, 10 are from site II and the rest from among the mobile sodium ions which cannot be located by x-ray analysis. This result supports the well established fact that sodium ions of site I are most difficult to exchange. In LaX-58 sample, exchanged La^{3+} ions were occupying site II only and site I' was vacant upto this exchange level. In the other two samples, namely, LaX-79 and LaX-96, these cations were occupying site I' and II and we could not locate any La^{3+} ion at sites I and V., as is reported by some other workers [50,32]. Reported site I

occupancy by La^{3+} ions is in the case of dehydrated samples but as our samples were hydrated so zero occupancy factor at site I is quite reasonable. Olson et al. [32] have reported four La^{3+} ions at site V. This works out to an occupancy factor of 0.25 for the site V and would give rise to low electron density for this position. Our temperature factors for the exchanged and even for the parent zeolite are high, indicating that our sample, even to start with, were somewhat less ordered, which would mean still lower contribution to the intensity of reflections and hence there may not be detected. Second reason for zero occupancy of site V can be the intermediate heat treatment done in our ion-exchange process. It may be possible that La^{3+} ions of site V have migrated to some interior site like II and I'.

Total number of La^{3+} ions located by x-ray analysis of different samples are given in table 5.5. One quite surprising and unexpected finding is that only 13.12 La^{3+} ions could be located for LaX-96 sample, while for LaX-79 this number was 25.56. But actually (Table 5.1) these are more lanthanum ions per unit cell (27.5 La^{3+} ions) in this sample as to those present in latter case (22.6 La^{3+} ions). Possible reasons for this could be -

1. After certain degree of exchange (around 80 per cent) La^{3+} ions entering the crystal lattice may have forced some of the lanthanum ions already sitting

at sites I' and II, to come out to the supercages. The reason behind this movement from sites I' and II to supercage may be that by presence of some La^{3+} ions in supercages, the potential energy equilibrium is shifted in such a fashion that supercage sites become more favourable for La^{3+} ions. These La^{3+} ions of the supercage may not be situated at any fixed position and are in a mobile state. They cannot be located by x-ray analysis as is the case with mobile Na^+ ions in the parent zeolite NaX [31, 37].

2. The other possible reason is that we used the same temperature factors for the atoms as were fixed for LaX-79 samples. As some of the temperature factors were becoming negative when they were allowed to vary, those were fixed arbitrarily by taking the average of temperature factors for the similar type of atoms and site positions. Therefore temperature factors used in LaX-96 sample refinement might have been lower than the actual temperature factor required for that sample, since the replacement of Na^+ by La^{3+} is likely to result in an increase in temperature factors. As occupancy factors are inversely related to temperature factors, by using actual temperature factor one can expect to get higher occupancy factor. But with the limited

powder data there is no reliable method of estimating temperature factors independently, so no firm conclusion could be drawn.

Bond lengths and angles calculated for our samples are not in very good agreement with reported data [30,31,37]. In general, average of both T-O and O-O bond lengths are higher and the average of bond angles (O-T-O and T-O-T) are lower than the reported data. Bond lengths and angles also vary with degree of exchange which is a indication of distortions produced by ion-exchange. It can be noticed (Table 5.7) that average value of bond lengths increase upto 79 per cent exchange level and then there is slight decrease. On the other hand, average value of bond angles first decrease upto 79 per cent degree of exchange and afterwards it increase. These variations may be due to inaccuracy of data obtained by less accurate powder method and use of old counter or due to some sort of lack of order in the crystal structure of the original sample supplied by the manufacturers. Firm conclusions, however, can be only drawn on the basis of further study with more accurate intensity data obtained from a single crystal.

Reliability indices (R) given in Table 5.5 are satisfactory, keeping in mind the fact that we used the R based on $|F|^2$ and the powder method. For powder method data of Shoemaker et al. [31] lowest value of R obtained was 0.36

(based on $|F|^2$) which is higher than values obtained in this work. Shoemaker et al. have also used arbitrary temperature factors (around 7.5) for fast convergence and to lower the value of R. Temperature factors obtained in this work are in the same range.

CHAPTER 6

CONCLUSIONS AND RECOMMENDATIONS

6.1 Conclusions: Zeolite 13X was ion exchanged with rare earth (La^{3+}) or transition metal (Ni^{2+}) to develop a better catalyst for hydrocracking of Assam crude residue. These catalysts were characterized by using DTA, TG, Surface Area, Pore Volume, Pore Size Distribution and detailed x-ray analysis including least square refinement. Based on the results discussed in previous chapters following conclusions were derived:

1. Lanthanum exchanged (LaX) zeolite turned out to be a suitable catalyst for hydrocracking of Assam crude residue. Its activity increased with increasing degree of ion-exchange and maximum lanthanum exchanged catalyst, LaX-96, was shown to be most suitable.
2. Some of the Lanthanum ions in LaX-96 sample may be in the more accessible supercage sites and are mobile in nature. This peculiarity of the state of the lanthanum ions resulted in highly acidic and hence most active catalyst.
3. The Na^+ ions located at site II and in supercage (mobile ions) are exchanged easily compared to those situated at site I. Lanthanum ions most preferable site is site II and next to it is site I'.

4. Nickel exchanged catalyst does not show very good activity due to the partial loss of the crystalline structure of the catalyst, although nickel is well known as a hydrogenating catalyst.
5. Powder x-ray analysis is not a very accurate method of studying effect of degree of exchange on crystal structure because of its various limitations. Single crystal analysis would be more suitable if the single crystals are available.

6.2 Recommendations:

Because of the non-availability of single crystals, x-ray analysis was carried out by using the powder-method. For more accurate study one should try to grow single crystals and use single crystal x-ray analysis method.

As temperature factors and occupancy factors are highly correlated with each other so one should take extra precautions to determine the temperature factors as accurately as possible by using some independent method like Wilson's plot. Use of anisotropic temperature factors with single crystal data is expected to give more reliable results.

Many important changes were noticed around 80 per cent exchange level for lanthanum exchanged samples. So the study of more number of samples between 80 and 96 per cent exchange region can give better understanding of ion-exchange process.

REFERENCE

- [1] Choudhary, N., Saraf, D.N., Ind. Eng. Chem., Prod. Res. Dev., 14(2), 74 (1975).
- [2] Pickert, P.E., Rabe, J.A., Dempsey, E., Shomaker, V., Proc. 3rd Int. Congr. Catalysis, 1, 714 (1965).
- [3] Kerr, G.T., J. Phys. Chem., 72, 2594 (1968).
- [4] Ibid, 73, 2780 (1969).
- [5] Peri, J.B., Proc. 5th Int. Congr. Catalysis, 1, 329 (1973).
- [6] Beaumont, R., Barthomeuf, D., J. Catal., 26, 218 (1972).
- [7] Beaumont, R., Barthomeuf, D., Trambouze, Y., Advan. Chem., Ser., 102, 327 (1971).
- [8] Kerr, G.T., Advan. Chem. Ser., 121, 219 (1973).
- [9] McDaniel, C.V., Maher, P.K., Conf. Mol. Sieves, Society of Chemical Industry, London (1967).
- [10] Ambs, W.J., Flank, W.H., J. Catal., 14, 118 (1969).
- [11] Kolesnikov, I.M., Panchenkov, G.M., Tretyakov, V.A., Russ. J. Phys. Chem., 41, 587 (1967).
- [12] Lapidus, A.L., Isakov, Y.I., Rudakova, L.N., Minachev, K.M., Eidus, Y.T., Bull. Acad. Sci. USSR, Div. Chem. Sci., 21, 1848 (1972).
- [13] Dempsey, E., in 'Molecular sieves', Society of the Chemical Industry, London, 2, 1968.
- [14] Way, J.T., J. Roy. Agri. Soc., 11, 313 (1850).
- [15] Barrer, R.M., Davies, J.A., Rees, L.V.C., J. Inorg. Nucl. Chem., 31, 2599 (1969).
- [16] Breck, D.W., 'Zeolite Molecular Sieves', Wiley-Intersciences, New York, 1974.

- [17] Sherry, H.S., *Advan.Chem.Ser.*, 101, 350 (1971).
- [18] Barrer, R.M., Davies, J.A., Rees, L.V.C., *J. Inorg. Nucl. Chem.*, 30, 3333 (1968).
- [19] *Ibid*, 31, 2599 (1969).
- [20] *Ibid*, 28, 629 (1966).
- [21] Sherry, H.S., *J. Phys.Chem.*, 70, 1158 (1966).
- [22] Theng, B.K.G., Vansant, E., Uytterhoeven, J.B., *Trans. Faraday Soc.*, 64, 3370 (1968).
- [23] Pauling, L., 'The nature of Chemical Bond', 3rd Edition, Cornell Univ. Press, Ithaca, 1960.
- [24] Smith, J.V., *Mineral. Soc. Am. Spec. Paper No.1*, 1963.
- [25] Mier, W.M., *Proc. Intern.Sym. Mol.Sieves*, 1st, London, 10(1968).
- [26] Damour, A., *Ann. Mines*, 1, 395 (1842).
- [27] Barrer, R.M., Bultitude, F.W., Sutherland, J.W., *Trans. Faraday. Soc.*, 53, 1111 (1957).
- [28] Kerr, G.T., Shipman, G.F., *J. Phys. Chem.*, 72, 3071 (1968).
- [29] Breck, D.W., 'Zeolite Molecular Sieves', Wiley-Interscience, New York, 1974.
- [30] Smith, J.V., *Advan. Chem.Ser.*, 101, 171 (1971).
- [31] Broussard, L., Shoemaker, D.P., *J.Am.Chem.Soc.*, 82, 1041 (1960).
- [32] Olson, D.H., Kokotailo, G.T., Charnell, J.F., *J. Colloid. Interface. Sci.*, 28, 305 (1968).
- [33] Bergerhoff, G., Baur, W.H., Nowacki, W., *News Jahrb. Mineral. Montash*, 193 (1958).
- [34] Reed, T.B., Breck, D.W., *J.Am.Chem.Soc.*, 78, 5972 (1956).

- [36] Olson, D.H., Dempsey, E., J. Catal., 13, 221 (1969).
- [37] Olson, D.H., J. Phys. Chem., 74, 2758 (1970).
- [38] Dempsey, E., Kuhl, G.H., Olson, D.H., J. Phys. Chem. 73, 387 (1969).
- [39] Eulenberger, G.R., Keil, J.G., Shoemaker, D.P., J. Phys. Chem., 71, 1812 (1967).
- [40] Sherry, H.S., J. Phys. Chem., 72, 4086 (1968).
- [41] Simpson, H.D., Steinfink, H., J. Am. Chem. Soc., 91, 6229 (1969).
- [42] Breck, D.W., J. Chem. Educ., 41, 678 (1964).
- [43] Olson, D.H., J. Phys. Chem., 72, 4366 (1968).
- [44] Dyer, A., Molyneux, A., J. Inorg. Nucl. Chem., 32, 2389 (1970).
- [45] Herd, A.C., Pope, C.G., J. Chem. Soc. Faraday Trans. I., 69, 833 (1973).
- [46] Pope, C.G., Thomas, M., J. Catal., 40, 67 (1975).
- [47] Serpinski, V.V., Rakhamukov, B.K., Minchev, K.M., Penchev, V., Izv. Akad. Nauk. SSSR. Ser. Khim., 23(2), 466 (1973), Mol. Sieve Abstr., 4(1), 23 (1974).
- [48] Gallezot, P., Imelik, B., J. Chim. Phys. Physicochim. Biol., 71(2), 155 (1974), (French).
- [49] Zhavoronkov, M.N., Zh. Struct. Khim., 13, 336 (1972) (Russ).
- [50] Bennett, J.M., Smith, J.V., Angell, C.L., Mater. Res. Bull., 4, 77 (1969).
- [51] Ibid, 3, 865 (1968).
- [52] Ibid, 4, 7 (1969).

- [53] Rabo, J.A., Angell, C.L., Schomaker, V., Intern. Congr. Catalysis. 4th, Moscow, 1968.
- [54] Bennett, J.M., Smith, J.V., Angell, C.L., Mater. Res. Bull., 4, 343 (1969).
- [55] Grimm, R.E., 'Clay Mineralogy', 2nd Ed., Chap. 9, McGraw-Hill, New York, 1970.
- [56] Barrer, R.M., Langley, D.A., J. Chem. Soc., 3804 (1958).
- [57] Barrer, R.M., Demy, A.F., J. Chem. Soc., 4684 (1964).
- [58] Breck, D.W., Flanigen, E.M., 'Molecular Sieves', Society of Chemical Industry, London, 47 (1968).
- [59] Barrer, R.M., Fender, B.E.F., J. Phys. Chem. Solids, 21, 1 (1961).
- [60] Murphy, J.R., Smith, M.R., Viens, C.H., Proc. Div. Refining, Am. Petrol. Institute, 50, 923 (1970).
- [61] Scott, J.W., Patterson, N.J., Proc. 7th World Petrol. Congr., 4, 97 (1967).
- [62] Scott, J.W., Bridge, A.G., Advan. Chem. Ser., 103, 113 (1971).
- [63] Voorhies, A., Jr., Smith, W.M., 'Advances in Petroleum Chemistry and Refining', Vol. 8, p.169, Interscience New York, 1964.
- [64] Chaudhary, N., Ph.D. Thesis, Chemical Engineering, Indian Institute of Technology, Kanpur, 1977.
- [65] McLachlan, Dan, Jr., 'X-ray Crystal Structure', p-63 McGraw-Hill, New York, 1957.
- [66] Cullity, B.D., 'Elements of x-ray Diffraction', Addison-Wesley Publishing Co., 1956.
- [67] Gupta, K.P., Bhat, S.P., 'X-ray Data Book', IIT-Kanpur.

- [68] International Tables for X-ray Crystallography, Vol.1
- [69] Ibid, Vol.2
- [70] Busing, W.R., Martin, K.O., Levy, H.A., 'ORFLS, A Fortran Crystallographic Least Squares Program', Oakridge National Laboratory, 1962.
- [71] Dwivedi, G.L., Ph.D. Thesis, Physics, IIT-Kanpur, 1972.
- [72] Buerger, J.M., 'Crystal Structure Analysis', p.629, John-Wiley and Sons, Inc., New York, 1967.
- [73] Darlow, S.F., Acta.Cryst., 683 (1960).
- [74] Coughlan, B., Carroll, W.M., JCS Faraday Trans. I., 72(9), 2016 (1976).
- [75] Olouna, H., Arai, Y., Ukihashi, H., Bull. Chem.Soc. Jap., 42, 2449 (1969).
- [76] Galbreath, R.B., VanaDriesen, R.P., Proc. 8th Wld. Congr. 4, 129 (1971).
- [77] Barrer, R.M., Proc.Chem.Soc. London, 99 (1958).

APPENDIX AX-RAY DIFFRACTION DATATABLE A.1: X-RAY DATA FOR NaX-100

$$a = 24.9954 \text{ \AA} \quad \text{Si/Al} = 1.23$$

$d(\text{\AA})$	I/I_0^δ per cent	$ F_o ^2$	$ F_c ^2$	hkl
14.6566	100	125000.00	126795.33	111
8.9162	30	24708.30	11174.99	220
7.5828	21	8791.67	16864.17	311
7.1380	3	3653.75	14.38	222
5.7536	39	16387.50	15957.10	331
5.5289	1	532.50	0.0	420
4.8217	10	6300.0	1248.50	511, 333
4.3229	19	16449.70	9847.38	440
3.9602	8	3307.02	4223.61	620
3.8176	60	26425.40	19939.51	533
3.7155	4	1504.40	8.43	622
3.3473	49	10882.10	6145.88	642
3.0562	9	3942.65	4344.98	733
2.9883	2	913.60	1803.42	820, 644
2.9478	16	9438.32	9524.15	822, 660
2.8892	49	19387.77	16321.16	751, 555
2.7968	19	8507.33	6446.34	840
2.7450	5	1557.10	709.62	753, 911
2.6672	19	8777.78	10431.19	664
2.6240	10	2317.42	4774.60	931

Table A.1 (contd)

$d(\text{\AA})$	I/I_0^δ per cent	F_o^2	F_c^2	hkl
2.4069	12	8380.68	8228.44	1022, 666
2.2106	8	7490.31	7045.39	800
2.1834	7	2176.47	5655.56	1131, 971, 955
2.1199	6	1777.13	303.00	1133, 973
1.9529	4	1562.60	6438.90	1242, 1080, 886
1.7890	3	1399.11	578.99	1264, 1400
1.7665	6	2893.27	2711.30	1086, 1420, 10100
1.7205	8	3006.32	1668.22	1193, 997
1.6027	9	4567.32	9837.48	1375, 1533, 11111, 9

$^\delta$ Value of I/I_0 are rounded off. For calculation of $|F_o|^2$ actual value of I/I_0 were first multiplied by 10^4 .

TABLE A.2: REPORTED DATA FOR NaX-100[13]

$$a = 24.93\text{\AA}$$

$$\text{Si/Al} = 1.25$$

d ° (Å)	I/I ₀ per cent	hkl
14.465	100	111
8.845	18	220
7.538	12	311
5.731	18	331
4.811	5	333, 511
4.419	9	440
4.226	1	531
3.946	4	620
3.808	21	533
3.765	3	622
3.603	1	444
3.500	1	711, 551
3.338	8	642
3.253	1	731, 553
3.051	4	733
2.944	9	822, 660
2.885	19	751, 555
2.794	8	840
2.743	2	911

TABLE A.3: X-RAY DATA FOR LaX-58

d (Å)	I/I_0^δ per cent	$ F_o ^2$	$ F_c ^2$	hkl
14.4413	100	125000.00	123842.74	111
8.8628	7	5600.00	3112.92	220
7.2310	4	4600.00	8203.08	222
6.2567	13	21833.30	22223.53	400
5.7425	48	20041.70	19549.23	331
4.8243	10	5984.38	3300.70	511, 333
4.4285	2	1627.60	4601.87	440
4.2402	3	716.84	3989.20	531
4.1617	1	790.23	638.11	442, 600
3.8184	85	37171.10	1925.72	533
3.5065	3	1687.83	1357.75	711, 551
3.3461	84	18528.40	13284.97	642
3.0583	2	761.20	2296.07	733
2.9535	23	13919.41	2998.65	822, 660
2.8929	53	20608.40	23829.32	751, 555
2.8002	39	17765.60	20549.51	840
2.7549	2	542.59	146.94	911, 753
2.6703	21	9826.39	4608.50	664
2.6255	18	4260.30	2795.82	931
2.5559	16	7537.45	6781.41	844
2.4555	4	1182.45	20208.02	1020, 862
2.4113	9	6548.30	5689.61	666, 1022

Table A.3 (contd)

d (Å)	I/I_o^{δ} per cent	$ F_o ^2$	$ F_c ^2$	hkl
2.2919	2	350.56	1455.99	1042
2.2567	2	869.70	1193.62	1111, 775
2.2142	25	23691.90	23303.81	880
2.1890	12	3576.48	4355.88	1131, 971, 955
2.1227	13	4134.00	1976.31	1133, 973
2.0668	2	797.20	809.01	1151, 777
1.9565	6	2099.85	1306.46	1242, 1080, 885
1.9099	2	853.66	7358.72	1171, 1155, 993, 1311
1.8887	3	1280.86	4936.71	1244
1.8715	33	868.52	3463.04	1331, 1173, 997
1.7935	3	1262.96	2.38	1264, 1400
1.7715	15	6971.07	4870.73	10100, 1086, 1420
1.7244	7	2341.78	5075.21	1193, 997,
1.6066	6	2758.16	12770.69	1533, 1375, 11111, 999
1.5420	1	862.01	3785.71	1622, 1482, 10108
1.5314	2	861.22	1808.08	1377, 11115
1.5189	6	3175.0	2856.98	1288, 1640
1.4771	6	4222.98	6123.89	1644, 12120
1.4564	5	1602.74	1326.49	1662, 14100, 1486
1.3831	5	2913.75	1139.52	1680
1.3145	4	2285.72	5432.90	1775, 13135, 1911, 111111

^δ Values of I/I_o are rounded off. For calculation of $|F_o|^2$ actual value of I/I_o were first multiplied by 10^4 .

TABLE A.4: X-RAY DATA FOR LaX-79

d (Å)	I/I_0^δ per cent	$ F_o ^2$	$ F_c ^2$	hkl
1	2	3	4	5
14.5362	100	125000.00	124803.00	111
8.8894	11	8961.67	6702.02	220
7.2427	14	17500.00	17171.58	222
4.8088	8	4625.00	2958.10	511, 333
4.1713	34	23472.10	22016.55	442, 600
3.8144	52	22719.30	22693.72	533
3.5065	7	2916.66	1143.36	711, 551
3.3473	12	2637.41	3744.41	642
3.2608	7	2068.55	7380.89	533, 731
3.1318	3	5483.97	6306.78	800
3.0359	8	3727.60	2230.85	733
2.9497	14	8206.52	9069.26	822, 660
2.8711	7	2857.14	1835.79	555, 751
2.8011	9	4175.82	3439.46	840
2.7491	12	3742.28	6256.62	911, 753
2.6710	4	2004.63	2122.19	664
2.6255	9	3412.58	499.46	931
2.5150	6	1271.40	2035.57	755, 771, 933
2.4552	10	3285.98	2125.18	1020, 862
2.4201	4	1248.11	6096.28	951, 773
2.2132	14	13255.80	13582.56	880

Table A.4 (contd)

1	2	3	4	5
2.1860	14	4132.35	3842.63	1131, 971, 955
2.1463	3	1370.59	2203.29	1060, 866
2.1232	5	1692.80	1903.62	973, 1133
1.9549	9	3486.70	5812.48	1242, 886, 1080
1.7890	8	3680.58	122.53	1264, 1400
1.7703	5	2034.36	5860.25	1086, 1420, 1010
1.6053	8	3846.11	1823.47	1375, 1533, 11111, 999

^δ Values of I/I_0 are rounded off. For calculation of F_0^2 actual value of I/I_0 were first multiplied by 10^4 .

TABLE A.5: X-RAY DATA FOR LaX-96

d (Å)	I/I_0^δ per cent	$ F_o ^2$	$ F_c ^2$	hkl
14.5124	100	125000.00	124198.00	111
8.8628	11	8958.33	9482.27	220
7.2310	13	16600.00	16065.71	222
5.7722	3	1387.50	2535.32	331
4.8165	8	5175.0	5426.68	511, 333
4.4285	3	2252.60	433.73	440
4.2223	4	919.50	29.00	531
4.1704	10	7054.67	4583.57	442, 600
3.8160	59	25986.80	26758.59	533
3.5038	8	3346.56	2143.25	711, 551
3.3436	9	1879.43	2211.41	642
3.2561.	4	1222.65	4294.70	731, 553
3.1393	3	5250.90	6218.31	800
3.0349	5	2347.67	2221.37	733
2.9469	11	6764.34	5607.82	822, 660
2.8811	4	1562.39	2504.58	751, 555
2.7972	6	2605.31	1668.19	840
2.7467	13	4037.00	1801.74	911, 753
2.6672	3	1214.81	231.92	664
2.6232	8	1816.48	25.50	931
2.5516	1	566.48	1148.83	844
2.5156	4	1850.28	5292.58	933, 771, 755

Table A.5 (contd)

1	2	3	4	5
2.4529	6	1941.28	1218.65	1020, 862
2.4163	3	2065.34	3841.32	1022, 666
2.2116	8	7848.84	7985.69	880
2.1855	6	1692.94	1628.88	1131, 971, 955
2.1463	1	593.63	3869.92	1060, 866
2.1227	3	908.50	2240.94	973, 1133
2.0646	3	1066.33	3234.00	1151, 777
2.0102	2	532.12	4412.43	1153, 975
1.9545	6	2791.90	3558.08	1242, 1080, 886
1.7894	4	2515.63	1625.77	1264, 1400
1.7696	3	1123.42	3907.49	1420, 10100, 1086
1.7557	3	691.72	2330.87	1353, 1191
1.7217	1	434.84	1707.86	1193, 997
1.6923	1	237.18	3339.54	1371, 1355, 1177
1.6053	4	1796.89	2945.05	1533, 1375, 11111, 999
1.5404	1	430.83	1676.68	1622, 1482, 10108
1.3115	1	262.89	3036.07	1911, 1775, 13135, 111111
1.3037	0.5	118.14	878.22	15115, 13119, 1931, 1791
1.2578	2	864.73	717.86	1866
1.2452	1	195.00	251.18	1884, 16122, 12148, 2020

^δ Values of I/I_0 are rounded off. For calculation of $|F_0|^2$ actual value of I/I_0 were first multiplied by 10^4 .

TABLE A.6: X-RAY DATA FOR NiX - 80

d_o (Å)	I/I_o	hkl
14.4178	84	111
8.8187	18	220
7.5635	9	311
6.3032	5	400
5.7057	55	331
4.7959	9	511, 333
4.4219	36	440
4.2583	5	531
3.9377	5	620
3.8015	63	533
3.3448	100	642
3.0491	10	733
2.9402	17	822, 660
2.8793	39	751, 555
2.7908	14	840
2.6610	16	664
2.3995	11	(10,2,2),(6,6,6)
2.3123	5	(10,4,0),(8,6,4)
2.2813	5	(10,4,2)
2.2475	7	(11,1,1),(775)
2.2257	2	880
2.2008	5	(11,3,1),(9,7,1),(9,5,5)
2.1270	3	(11,3,3),(9,7,3)
2.8248	6	(13,3,3),(995)
1.7504	4	(13,5,3),(11,9,1)

APPENDIX B

LISTING OF COMPUTER PROGRAMS

(with brief descriptions of data input)

B.1 Program for Bond Lengths and Angles Calculations:

This program was developed by Dwivedi [71]. Calculation of bond lengths and angles can be performed by this program. Standard deviations (s.d.) in them can also be determined if s.d. in coordinates are provided. This program can be used for triclinic, monoclinic, orthorhombic, tetragonal and cubic systems.

For a given unit cell dimension, this program does calculations for different sets of atoms. In each set of atoms it calculates all possible bond lengths among the atoms. If angle calculations are also to be done, then IANGL=1 is given and the NANGL should be assigned the number of angles to be calculated. More input data required are described below:

Input Data:

1. Cell parameter card FORMAT (6F10.5)
One card only

Columns

1-10	A i.e. cell parameter	a in Angstroms
11-20	B i.e. cell parameter	b in Angstroms
21-30	C i.e. cell parameter	c in Angstroms
31-40	ALFA i.e. cell parameter	α in degrees
41-50	BETA i.e. cell parameter	β in degrees
51-60	GAMA i.e. cell parameter	γ in degrees

2. Instruction card for number of sets: `FORMAT (I2)`

Column

- 1-2 `NTIME`, indicator of number of sets i.e. the total number of group of atoms in the unit cell for which the calculation is to be done.

3. Input cards for each set

(a) Instruction card for first set `FORMAT(2I2,F12.4)`

Column

- 1-2 `NATOM`, integer indicating the number of atoms in the set

- 3-4 `ISD`, indicator for whether s.d. data are given or not.
 = 1 if s.d. data are given

 = 0 if no such data are given

- 5-16 `AR`, Value of Reliability Index `R`.

It is printed out with other results to indicate the stage of structure refinement at which the bond lengths and angles are calculated.

(b) Position parameter card: `FORMAT (A6,2TX,3F9.6)`

Number of these cards is equal to the value of `NATOM` in the set.

Column

- 1 - 6 `IDEN`, Punch name of the atoms for identification purpose

- 7 -27 Blank

- 28-36 `X`, Fractional x-coordinate of the atom

- 37-45 `Y`, Fractional Y-coordinate of the atom

- 46-54 `Z`, Fractional Z-coordinate of the atom

(c) Standard deviation card: FORMAT (9X,3F9.6)

Columns

1-9	Blank
10-18	DX , standard deviation in x.
19-27	DY , standard deviation in y.
28-36	DZ , standard deviation in z.

For ISD=1, each position parameter card should follow by a standard deviation card. For ISD=0 these s.d. cards are not required.

(d) Instruction card for angle calculation: FORMAT (2I5)

Column

1-5	IANGL = 1 if angle calculation is to be done = 0 if no such calculation is to be done
6-10	NANGL, equal to total number of angles to be calculated.

For IANGL = 0 leave this field as blank

(e) Angle selector card: FORMAT (3I2)

Number of these cards is equal to the value of NANGL column.

Column

1-2	J = Serial number of first atom defining the angle
3-4	K = Serial number of second atom defining the angle
5-6	L = Serial number of third atom defining the angle

Example:

Serial No.

Atom

1	
2	C(5)
3	C(3)
4	C(8)
	C(6)

If we want to calculate angle $C(5) - C(8) - C(6)$, then J, K and L should be assigned the values 1, 3 and 4 respectively.

4. Input cards for next set: Repeat input data cards for next set as given in para (3) till input data for all sets end.

B.2 Least Squares Refinement Program (ORFLS)

The listing of the program given here is same as developed by Levy [70]. The program performs successive cycles of refinement using full-matrix of normal equations. The main program (ORFLS) performs the basic operations associated with least squares refinement. Subroutine PRELIM serves to read the control informations and trial parameters for crystal structure. Scaled structure factors, their derivatives with trial parameters are calculated by subroutine CALC. Adjusted temperature factors are checked for the sign by subroutine TEST. Inversion of matrix, is done by subroutine DIVEDI[71]. For the atoms in special positions, subroutine PATCH, RESETX, RESETB (only when anisotropic temperature factors are used) perform the necessary modifications required from general positions. Listing of these subroutines written for our case are also given. Below is given description of input data changes made from original program. Glossary of symbols and other detailed information about input data are given by Levy [70].

1. Alphanumeric Labels Cards:

These input Hollerith informations are used to label each parameters at the time of the output of old and new parameters. Total number of these cards is three:

1st Card

FORMAT (12A6)

Columns

1-12	SCALE FACTOR
13-24	OVERALL B
25-36	FORM FACTOR
37-48	MULTIPLIER
49-60	X
61-72	Y

2nd Card

FORMAT (12A6)

Columns

1-12	Z
13-24	BETA(1,1)
25-36	BETA(2,2)
37-48	BETA(3,3)
49-60	BETA(1,2)
61-72	BETA(1,3)

3rd Card

Columns

1-12	BETA (2,3)
13-24	ATOMIC B

2. Title card

FORMAT (12A6)

Same as described by Levy [70]

3. Control Cards:

First Card

FORMAT (10I1)

Columns

1

IPRT, Indicates whether the calculated and observed structure factors are to be printed or not. If IPRT=0 then they will not be printed for any cycle. For IPRT=1 they can be printed for a particular cycle depending on the values given for IPRT1, IPRT2,etc.

2

IPRT1, If IPRT1=0, list of structure factors before first cycle of refinement will not be printed.

= 1 then they will be printed

3

IPRT2, = 0 then list before 2nd cycle of refinement will not be printed
= 2 Then they will be printed.

10

IPRT9 = 0 then list before 10th cycle of refinement will not be printed.
= 10 the list will be printed.

Second card

FORMAT (6I3)

Same as described by Levy [70]

Third card

FORMAT (7I3)

Same as described by Levy [70]

4. Scattering factor tables.

FORMAT (SF9.3)

Same as described by Levy [70]

5. Symmetry Cards:

FORMAT (F11.6, 2I2 F11.6, 2I2,
F11.6, 2I2)

Same as described by Levy [70]

6. Reciprocal Cell Data Card:

FORMAT (6F9.6)

Same as described by Levy [70]

7. Trial parameter cards: To be supplied only when IP=0

A. Scale factor cards

FORMAT (8F9.6)

Same as described by Levy [70]

B. Over-all temperature factor card:

FORMAT(F9.6)

Same as described by Levy [70]

C. Atom parameter cards: Two cards are required for each atom i in the asymmetric unit, where $I=1, 2, \dots, NA$.

First Card

FORMAT (A6, 3X, SF9.6)

Same as described by Levy [70]

Second Card

FORMAT (6F9.5)

Same as described by Levy [70]

8. Reflection data cards:

FORMAT (I1, F8.0, 5F9.0)

One card is needed for each reflection observed.

Same as described by Levy [70]

9. Observation termination card: FORMAT (I1,44X,5F9.0)

Column

1	1	as a sentinel for the end of the observation deck.
2-44		blank
45-54		q equal to 1 when single scale factor is used.
